Simulations of inflationary magnetogenesis and gravitational waves

Axel Brandenburg
(Nordita)

$$\left(\frac{\partial^2}{\partial\eta^2}+k^2-\frac{a''}{a}\right)\tilde{h}_{ij}=\frac{16\pi}{m_{\rm pl}^2}\,\frac{\tilde{T}_{ij}}{a},$$

$$T_{ij}=-B_iB_j-E_iE_j+a^2\partial_i\phi\partial_j\phi+\ldots$$

Why inflationary?

Larger length scales
Stronger GW field

$$\mathcal{E}_{\rm GW}^{\rm sat} \approx \left(q\mathcal{E}_{\rm M}^{\rm max}/k_{\rm peak}\right)^2$$

↑ efficiency

Numerical approaches

Time stepping

Length of time step

PDEs versus ODEs

Courant-Friedrich-Levy condition

Inflation versus radiation era

$$\partial_\tau^2\phi + 2\mathcal{H}\partial_\tau\phi - \boldsymbol{\nabla}^2\phi + a^2\frac{dV}{d\phi} = \frac{\alpha}{a^2 f}\boldsymbol{E}\cdot\boldsymbol{B},$$

$$\partial_\tau \boldsymbol{E} - \mathrm{rot}\,\boldsymbol{B} + \frac{\alpha}{f}\left(\partial_\tau\phi\boldsymbol{B} + \boldsymbol{\nabla}\phi\times\boldsymbol{E}\right) + \boldsymbol{J} = 0,$$

$$\boldsymbol{\nabla}\cdot\boldsymbol{E} = -\frac{\alpha}{f}\boldsymbol{\nabla}\phi\cdot\boldsymbol{B}, \quad \boldsymbol{\nabla}\cdot\boldsymbol{B} = 0,$$

$$\partial_\tau\boldsymbol{B} + \mathrm{rot}\,\boldsymbol{E} = 0,$$

$$\mathcal{H}^2 = \frac{8\pi}{3m_{\mathrm{Pl}}^2}a^2\left(\rho_\phi + \rho_E + \rho_B + \rho_\chi\right),$$

$$\boldsymbol{J} = \sigma_E\boldsymbol{E} + \sigma_B\boldsymbol{B}$$

$$\frac{\partial\ln\rho}{\partial t} = -\frac{4}{3}\left(\boldsymbol{\nabla}\cdot\boldsymbol{u} + \boldsymbol{u}\cdot\boldsymbol{\nabla}\ln\rho\right) + \frac{1}{\rho}\left[\boldsymbol{u}\cdot(\boldsymbol{J}\times\boldsymbol{B}) + \eta\boldsymbol{J}^2\right],$$

$$\frac{\partial\boldsymbol{u}}{\partial t} = -\boldsymbol{u}\cdot\boldsymbol{\nabla}\boldsymbol{u} + \frac{\boldsymbol{u}}{3}\left(\boldsymbol{\nabla}\cdot\boldsymbol{u} + \boldsymbol{u}\cdot\boldsymbol{\nabla}\ln\rho\right) + \frac{2}{\rho}\boldsymbol{\nabla}\cdot(\rho\nu\boldsymbol{S})$$
$$-\frac{1}{4}\boldsymbol{\nabla}\ln\rho - \frac{\boldsymbol{u}}{\rho}\left[\boldsymbol{u}\cdot(\boldsymbol{J}\times\boldsymbol{B}) + \eta\boldsymbol{J}^2\right] + \frac{3}{4\rho}\boldsymbol{J}\times\boldsymbol{B},$$

$$\frac{\partial\boldsymbol{B}}{\partial t} = \boldsymbol{\nabla}\times\left(\boldsymbol{u}\times\boldsymbol{B} - \eta\boldsymbol{J} + \boldsymbol{\mathcal{F}}\right), \qquad \boldsymbol{J} = \boldsymbol{\nabla}\times\boldsymbol{B}.$$

Inverse Cascade

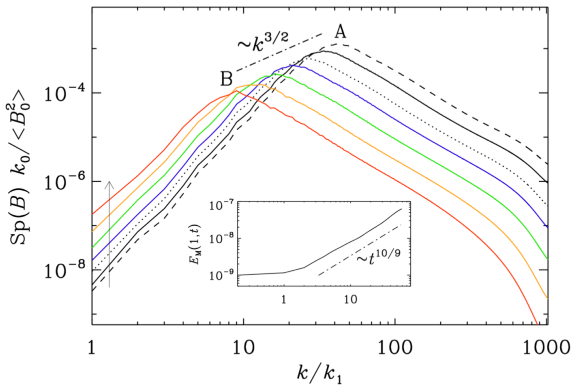

Magnetic field: link between very early universe and today

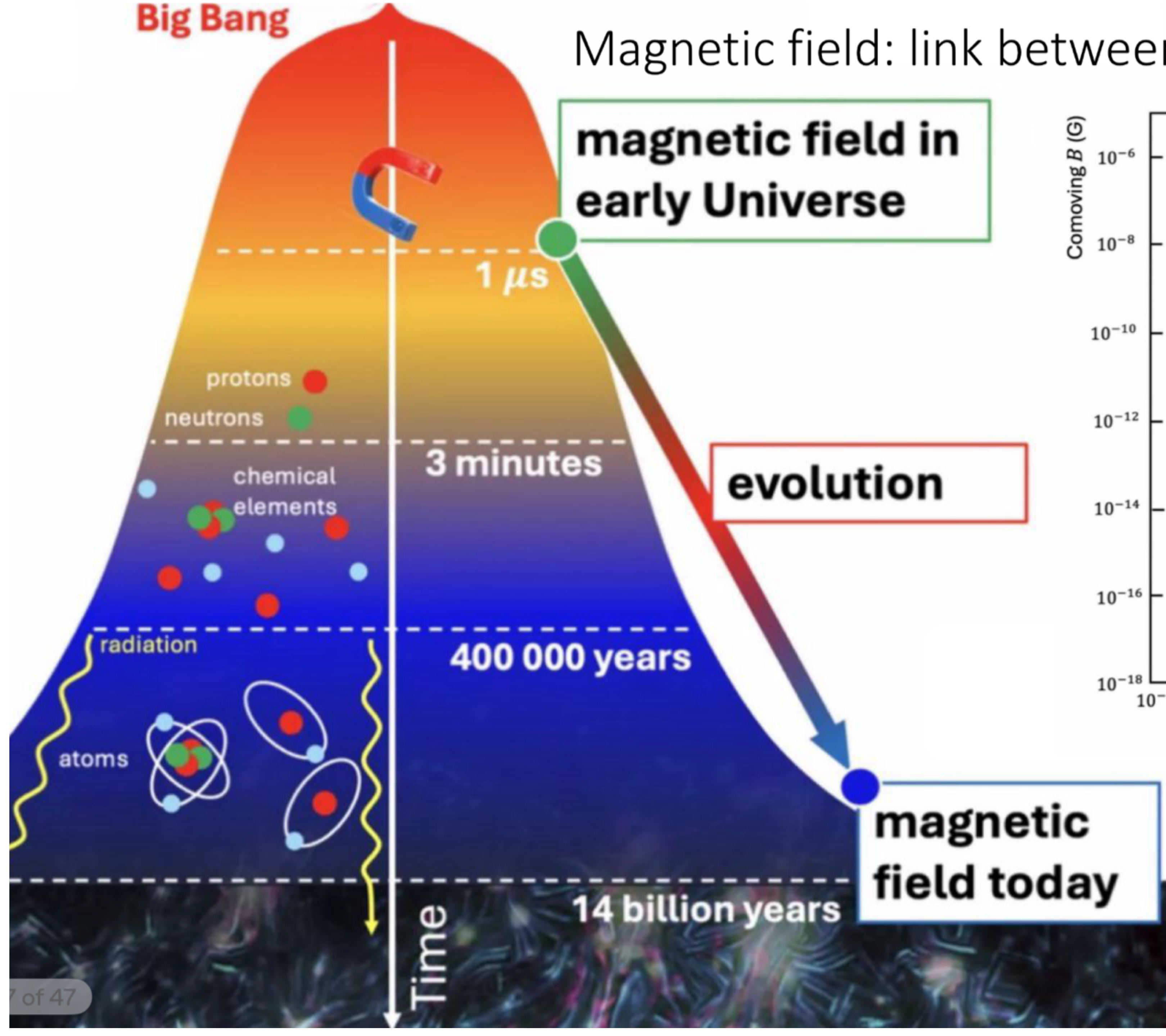

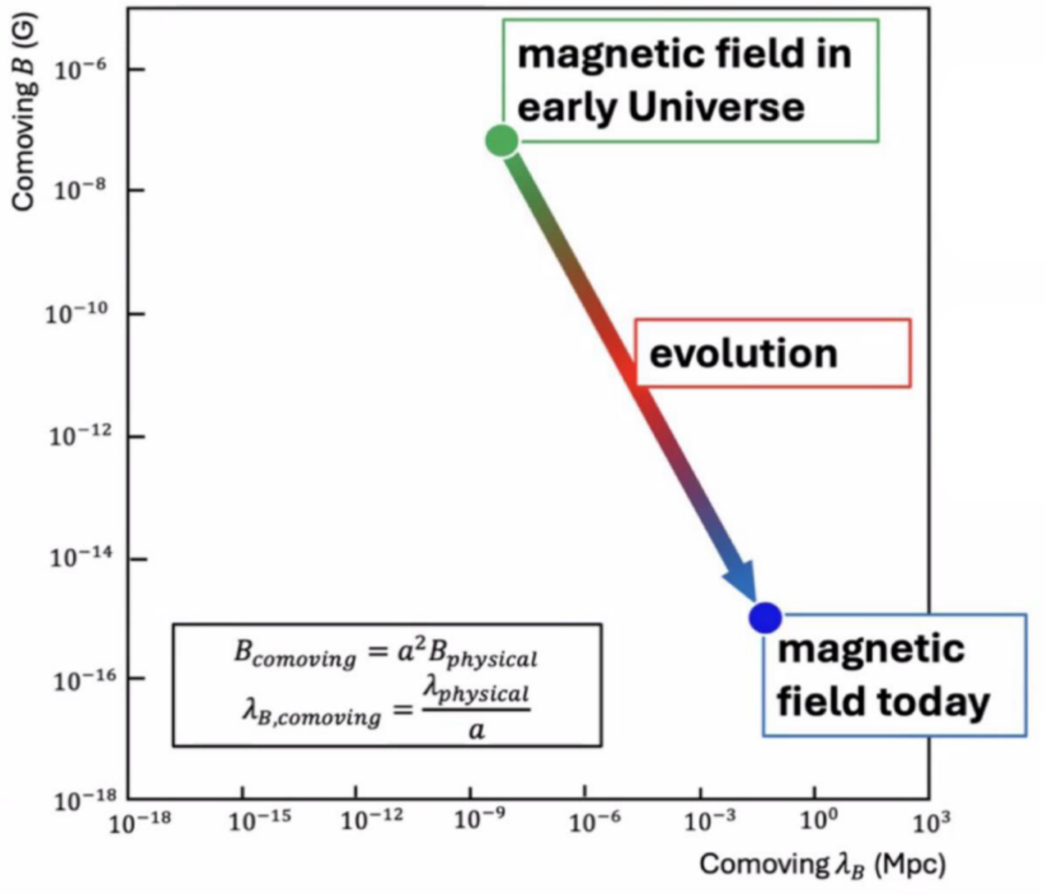

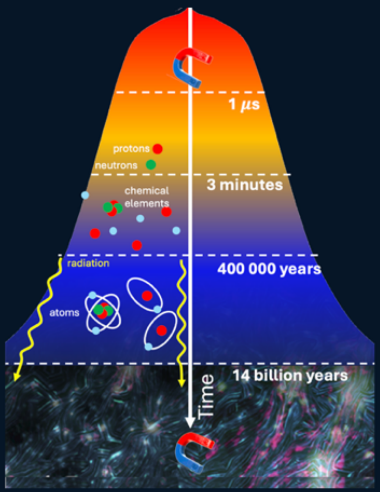

Nordita Winter School 2026 - Cosmological Magnetic Fields: Generation, Observation, and Modeling

https://indico.fysik.su.se/event/8554/

12-23 Jan 2026 — Albano Building 3

Enter your search term

Venue

Registration, 12 Jan. 09:15: Albano Campus, House 3, floor 6 (Nordita building)

Lectures: Room 4205, Conference Center, Albano Campus, House 3, floor 4 (Nordita building)

Workspaces: Use the open desks throughout floor 6 and floor 5 (east).

Coffee: Help yourself to free coffee in Nordita's kitchens on floor 6 and floor 5 (east).

Application to the school is now open, and will close on Oct 15, 2025.

Lectures and topics:
- Cosmological magnetic field theory
- Cosmological magnetic field observations
- Evolution before recombination, numerical approaches to magnetogenesis
- Evolution after recombination, basics of structure formation
- Hands-on and exercise sessions on data analysis, simulations with magneto-hydrodynamic code(s), theory

The deadline for registration is October 15, 2025.

Scope

Magnetic fields are omnipresent in the Universe, we find them in galaxies and galaxy clusers, in filaments and voids of the Large Scale Structure. The presence of magnetic fields in voids hints to the possibility that the initial fields have been generated in the early Universe, within the first micorseconds of the Universe history. Tracing the evolution of magnetic fields through the cosmological epochs is a challenging endeavour, and complex numerical simulations are used for this purpose. Several techniques from different domains of astronomy: radio, microwave, gamma-rays, gravitational waves, are used to probe cosmological magnetic fields at different epochs and scales.

(magneto) Hydrodynamic cascades in action

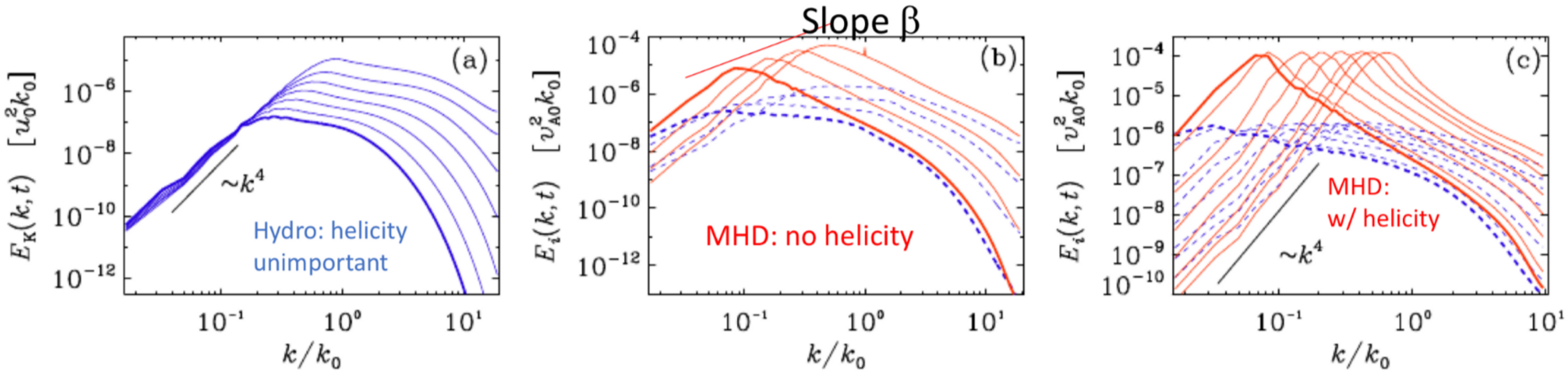

Forward and inverse cascades

What about gravitational waves?

Correspondence with (magnetohydrodynamic) turbulence

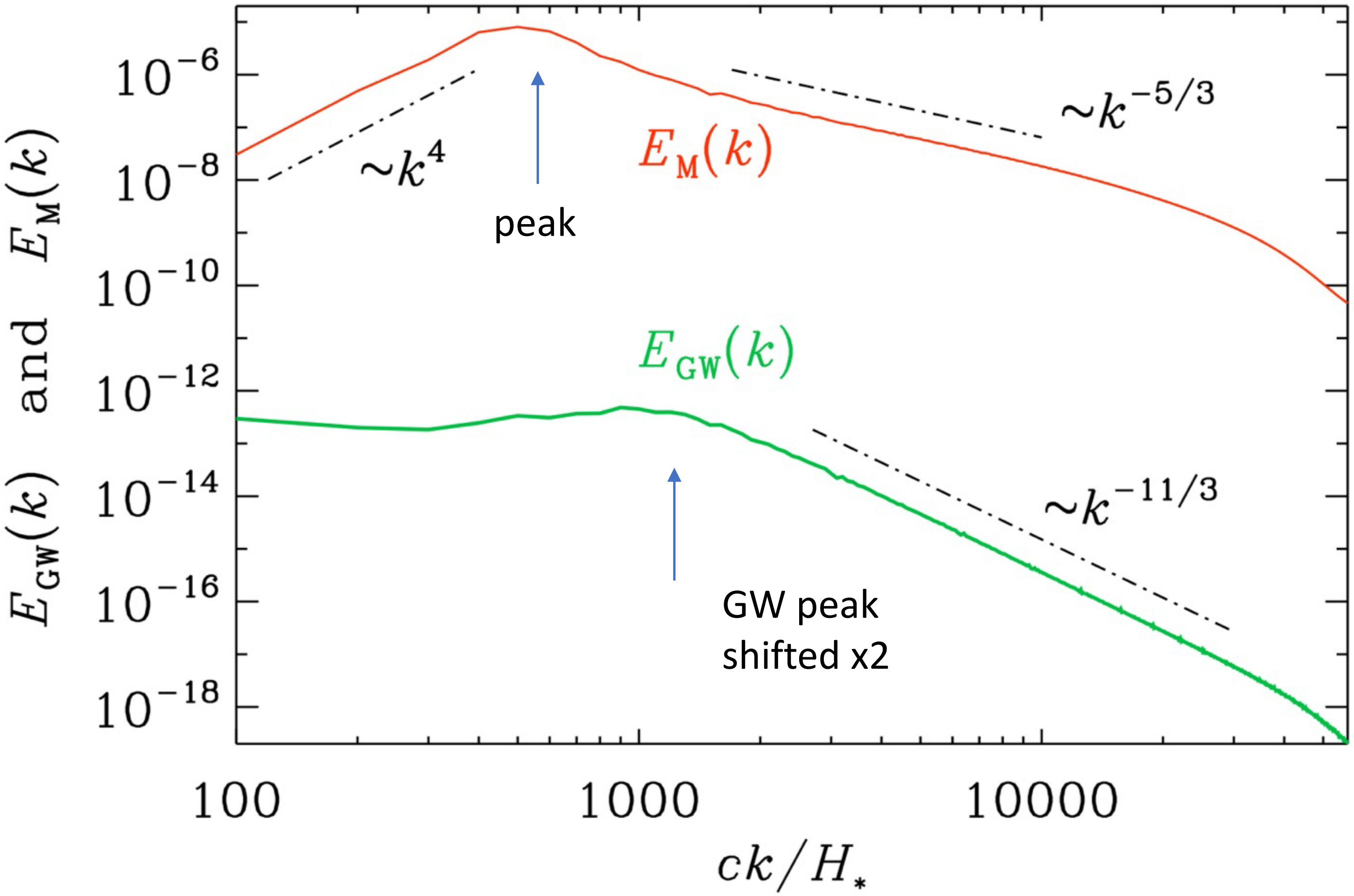

Roper Pol et al. (2020)

- Spectral energy per linear wavenumber interval
- $\Omega_{GW}(\ln k)=kE_{GW}$
- Forward cascade $k^{-5/3}$

$$\left(\partial_t^2 + 3H\partial_t - c^2\nabla^2\right) h_{ij}(\boldsymbol{x},t) = \frac{16\pi G}{c^2} T_{ij}^{\rm TT}(\boldsymbol{x},t)$$

- Relation between spectra:

$$\mathrm{Sp}(\dot{\mathbf{h}}) \approx k^2 \mathrm{Sp}(\mathbf{h}) \approx k^{-2} \mathrm{Sp}(\mathbf{T}),$$

GW slope by k^2 steeper
Peak at twice magnetic peak

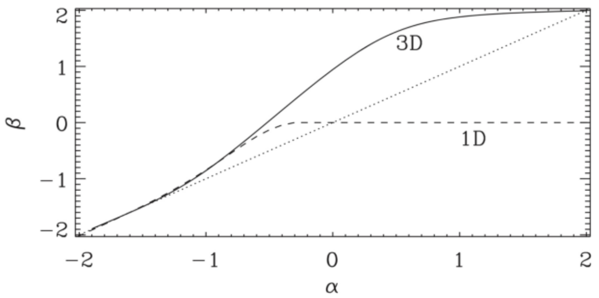

Numerical approaches

Time stepping

Length of time step

PDEs versus ODEs

Courant-Friedrich-Levy condition

Inaccuracy of "usual" 3rd order Runge-Kutta

$$\begin{pmatrix} h_{ij} \\ h'_{ij} \end{pmatrix}_{t+\delta t} \equiv \boldsymbol{q}_i, \quad \text{where} \quad \boldsymbol{q}_i = \boldsymbol{q}_{i-1} + \beta_i \boldsymbol{w}_i, \quad \boldsymbol{w}_i = \alpha_i \boldsymbol{w}_{i-1} + \delta t \boldsymbol{Q}_{i-1}, \quad \text{(approach I)}.$$

with $\alpha_1 = 0$, $\alpha_2 = -5/9$, $\alpha_3 = -153/128$, $\beta_1 = 1/3$, $\beta_2 = 15/16$, $\beta_3 = 8/15$, and

$$\boldsymbol{q}_{i-1} \equiv \begin{pmatrix} h_{ij} \\ h'_{ij} \end{pmatrix}_t, \quad \boldsymbol{Q}_{i-1} \equiv \begin{pmatrix} h'_{ij} \\ c^2 \nabla^2 h_{ij} + \mathcal{G} T_{ij} \end{pmatrix}_t.$$

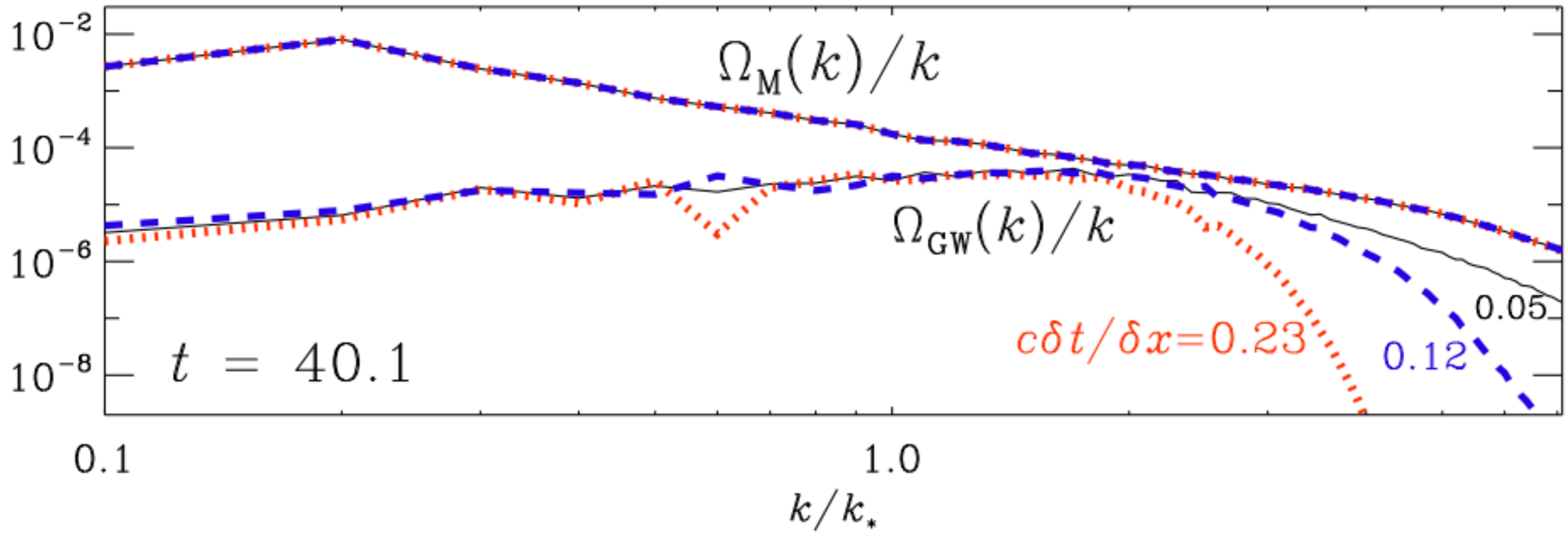

Alternative: exact solution for constant source between time steps

Consider: $$\ddot{h} + k^2 h = S$$

Solve as 2 first-order eqs

$$\begin{aligned} \dot{h} &= g \\ \ddot{h} \equiv \dot{g} &= -k^2 h + S \end{aligned}$$

General solution:

$$\begin{aligned} h &= +A\cos kt + B\sin kt + k^{-2}S \\ g &= -Ak\sin kt + Bk\cos kt, \end{aligned}$$

(h, g) at $t = 0$

$$\begin{aligned} A &= h - k^{-2}S \\ B &= k^{-1}g \end{aligned}$$

$$\begin{aligned} h(\delta t) &= +(h - k^{-2}S)\cos k\delta t + k^{-1}g\sin k\delta t + k^{-2}S \\ g(\delta t) &= -(h - k^{-2}S)k\sin k\delta t + k^{-1}gk\cos k\delta t, \end{aligned}$$

$$\begin{pmatrix} kh - k^{-1}S \\ g \end{pmatrix}_{\rm new} = \begin{pmatrix} \cos k\delta t & \sin k\delta t \\ -\sin k\delta t & \cos k\delta t \end{pmatrix} \begin{pmatrix} kh - k^{-1}S \\ g \end{pmatrix}_{\rm current}$$

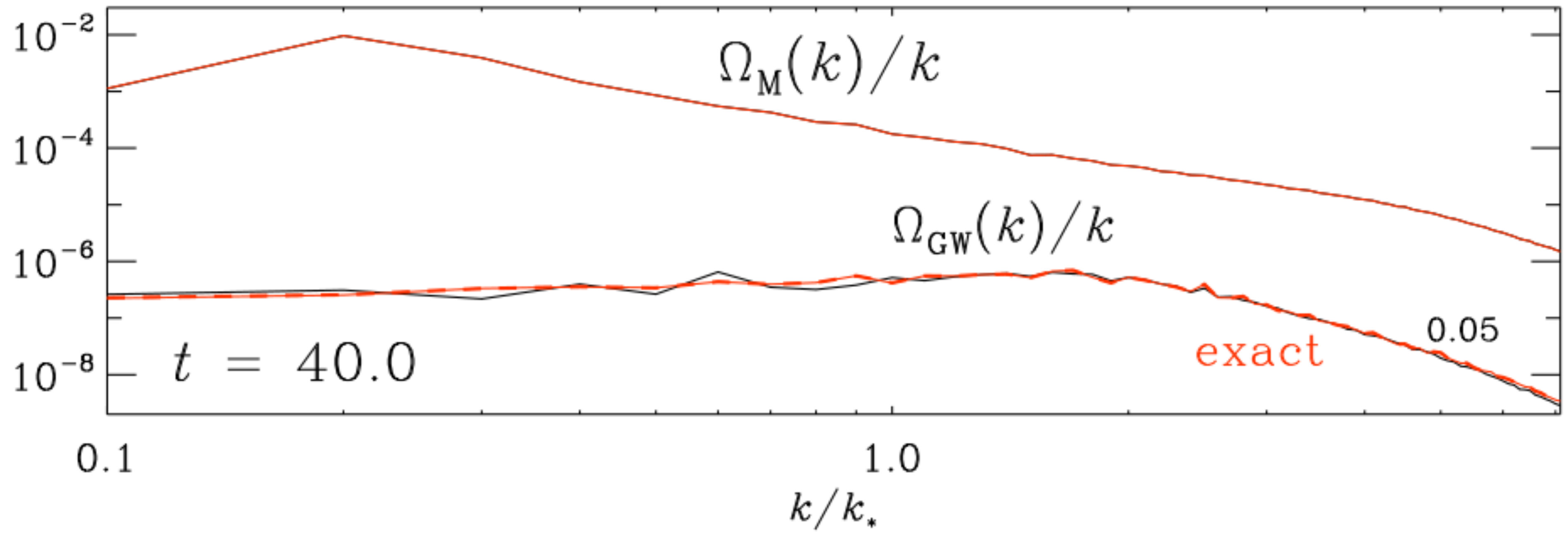

Dependence of accuracy on time step: only 1st order

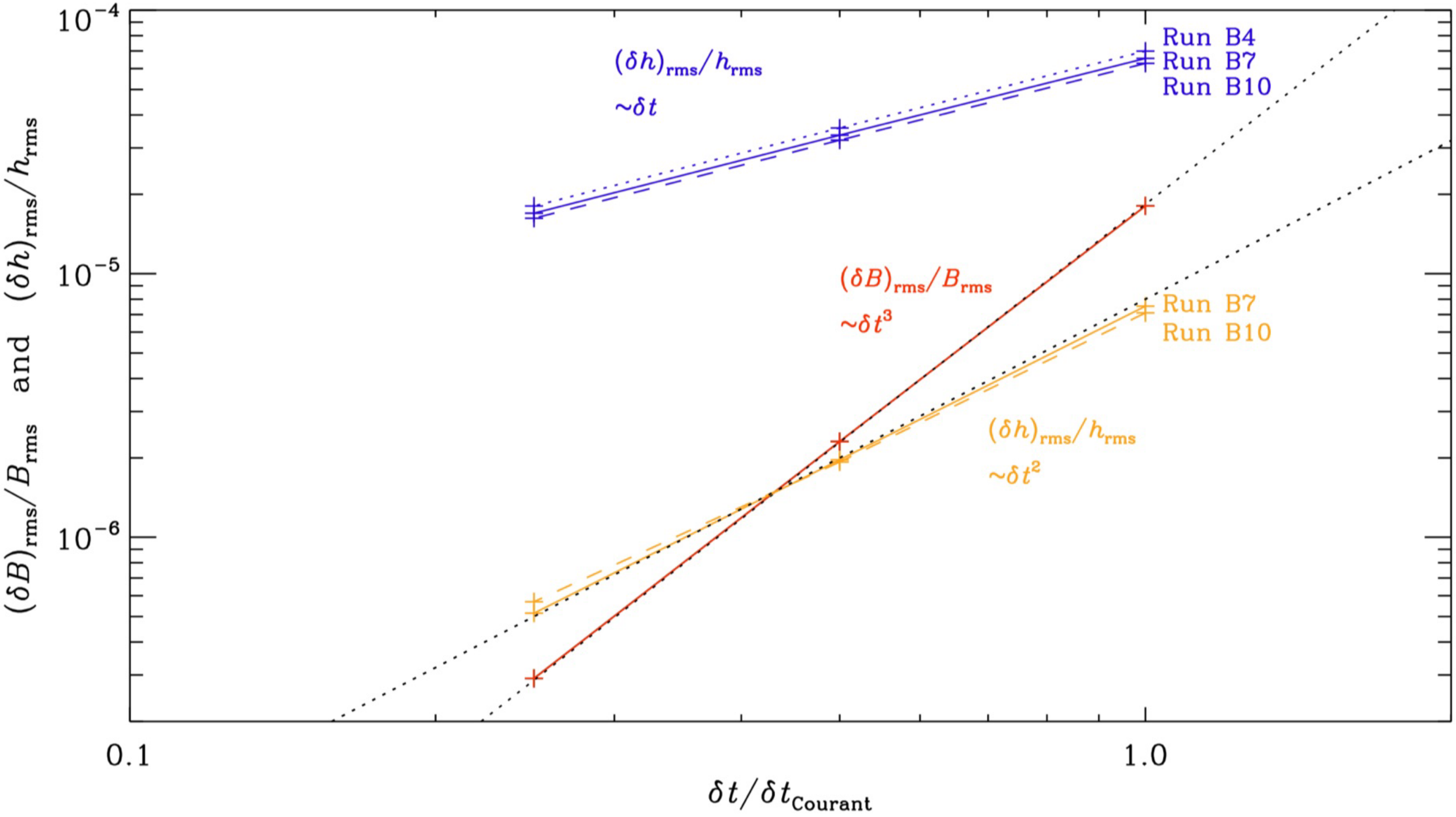

Allowing linear variations between time steps

Taylor expand:

$$\begin{aligned} h &= +A\cos kt + B\sin kt + k^{-2}(S_0 + \dot{S}_0\delta t) \\ g &= -Ak\sin kt + Bk\cos kt + k^{-2}\,\dot{S}_0 \end{aligned}$$

Modified update involving δS

$$\begin{pmatrix} kh - k^{-1}(S_0 + \delta S) \\ g - k^{-2}\delta S/\delta t \end{pmatrix}_{\text{new}} = \begin{pmatrix} \cos k\delta t & \sin k\delta t \\ -\sin k\delta t & \cos k\delta t \end{pmatrix} \begin{pmatrix} kh - k^{-1}S \\ g - k^{-2}\delta S/\delta t \end{pmatrix}_{\text{current}}$$

Additional update to make it 2nd order:

$$\begin{pmatrix} h \\ g \end{pmatrix}_{\text{2nd order}} = \ldots + \frac{\delta S}{k^2} \begin{pmatrix} [1 - (\sin k\delta t)/k\delta t] \\ (1 - \cos k\delta t)/\delta t \end{pmatrix}$$

→ Error decreases quadratically with decreasing time step dt

→ At no additional cost

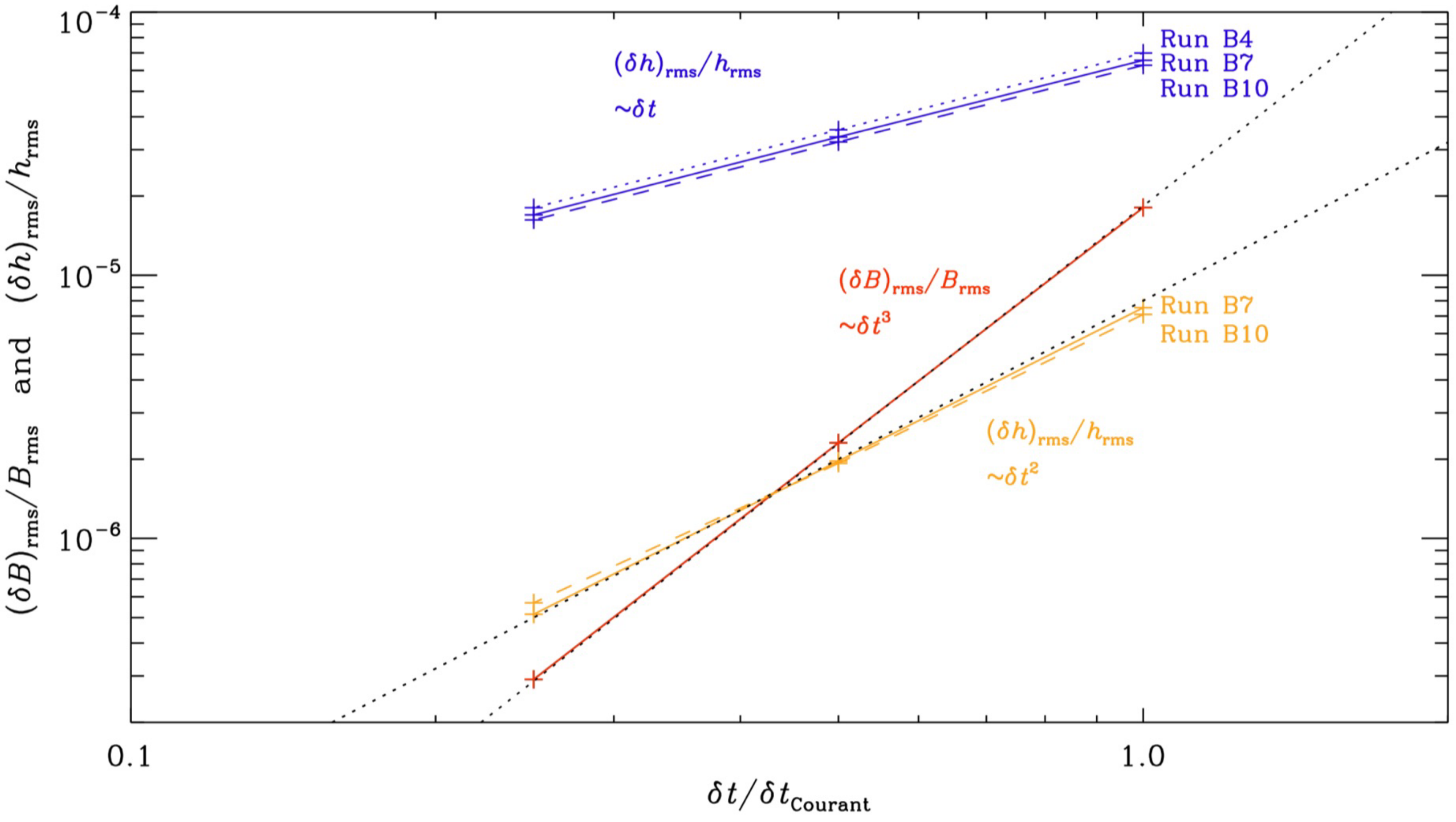

GW spectra from turbulent magnetic fields

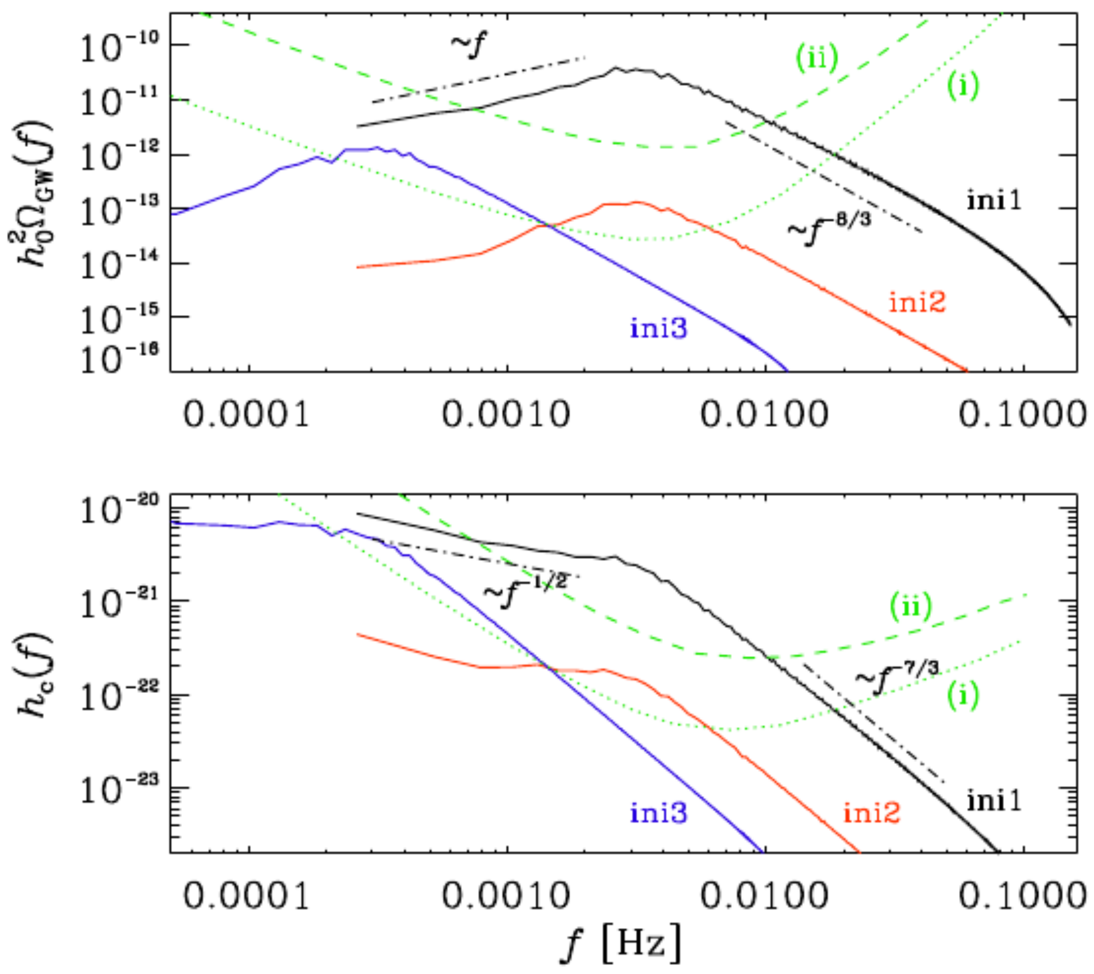

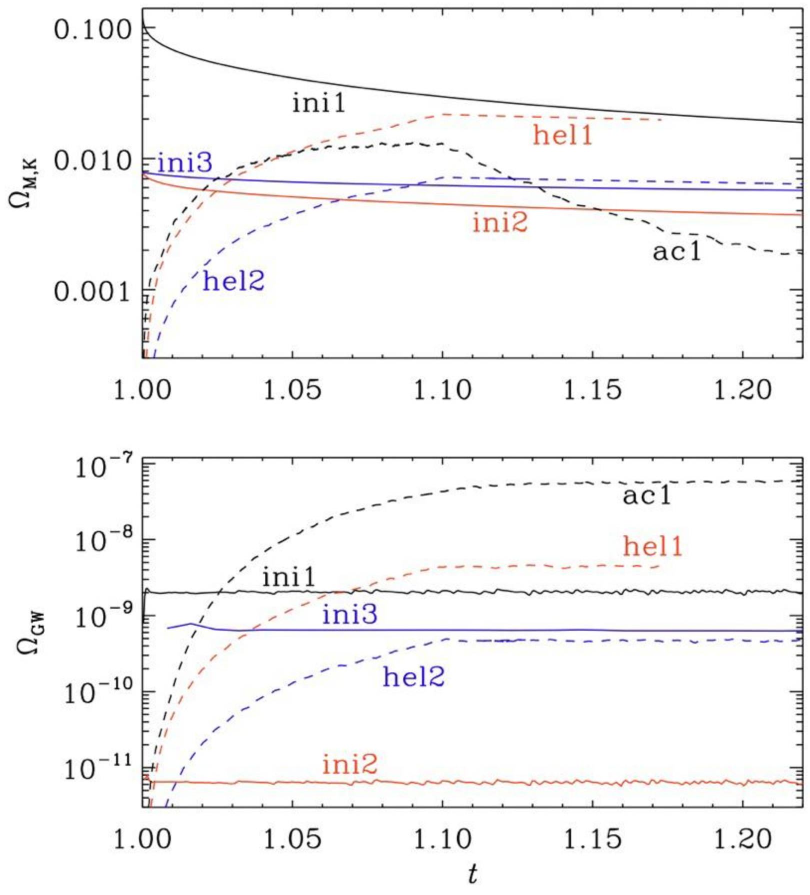

Roper Pol+20

- Magnetic energy decays
- GW energy does not!

GW energy depends quadratically on energy input & scale

Brandenburg+21

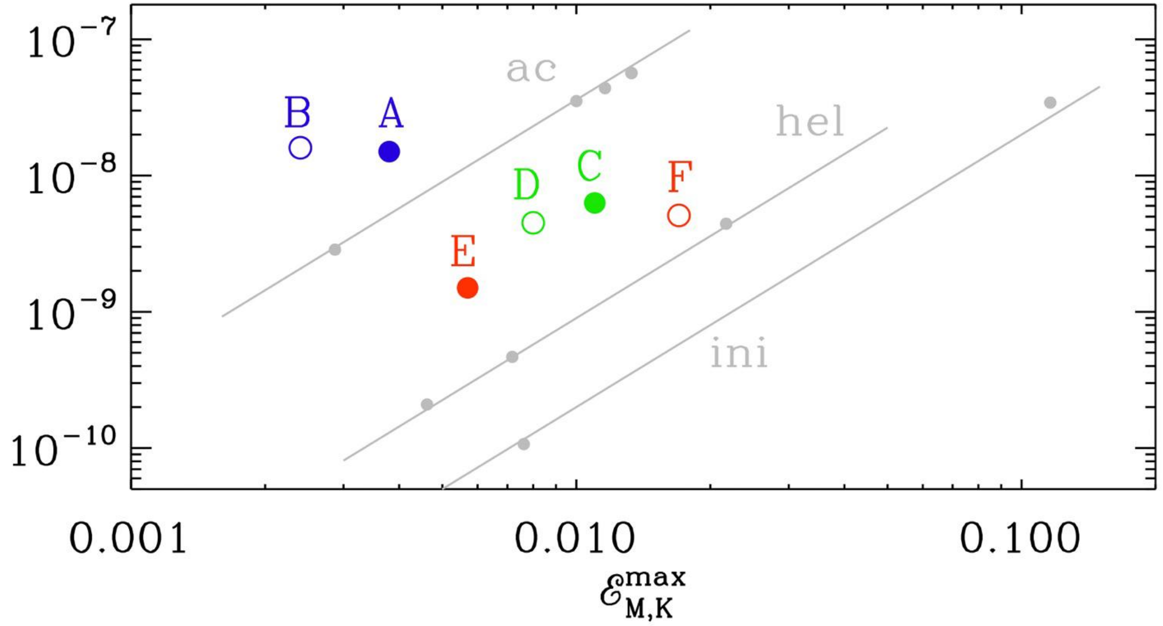

$$\mathcal{E}_{\rm GW}^{\rm sat} \approx (q\mathcal{E}_{\rm M}^{\rm max}/k_{\rm peak})^2$$

Acoustic turbulence most efficient (*q*~30)

Vortical turbulence less efficient (*q*<5)

Helical MHD turbulence even less efficient

Initiated turbulence least efficient

- Large-scale fields → more GW energy
- Generation at electroweak era: need strong fields
- Generation during inflation & reheating

Additional features for driven turbulence

- Bump for acoustic turbulence
  - Is actually real
  - First seen in sound-shell model
- Sharp cutoff to the right
  - controlled by initial peak
  - Subsequent build-up of turbulence has no effect anymore

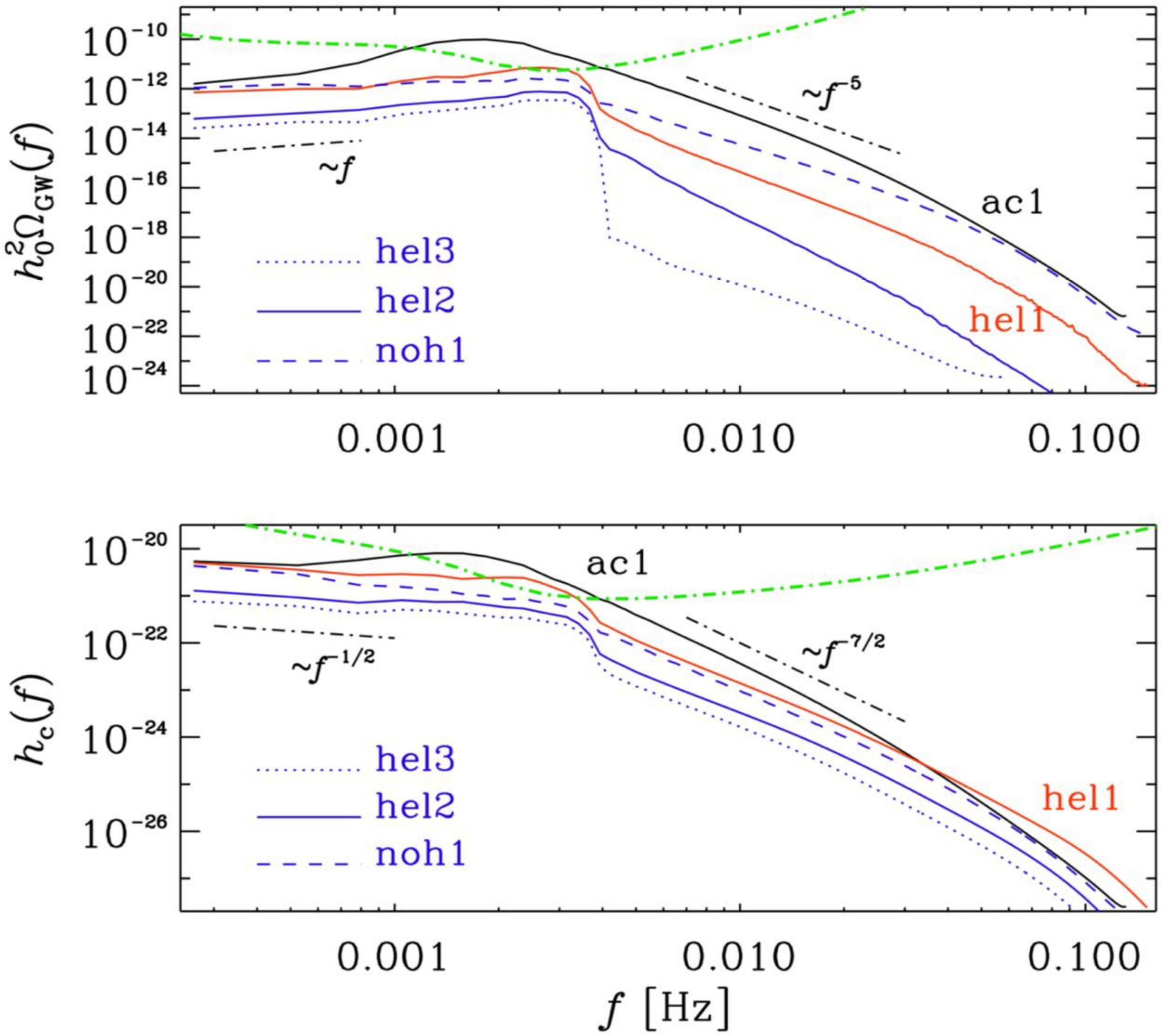

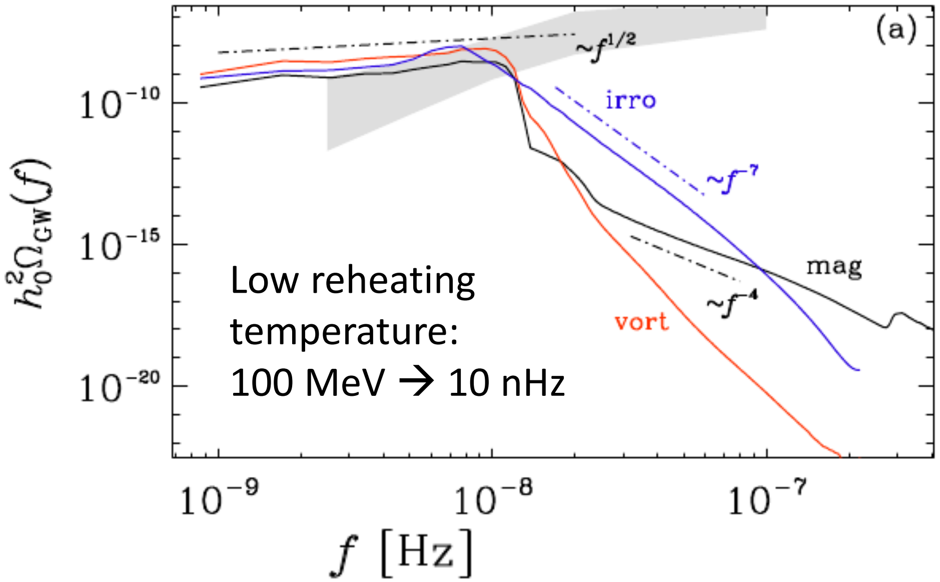

Circular polarization of gravitational waves from early-Universe helical turbulence

Tina Kahniashvili,[1,2,3,4,*] Axel Brandenburg,[5,6,2,1,†] Grigol Gogoberidze,[2,‡] Sayan Mandal,[7,2,§] and Alberto Roper Pol[8,2,∥]

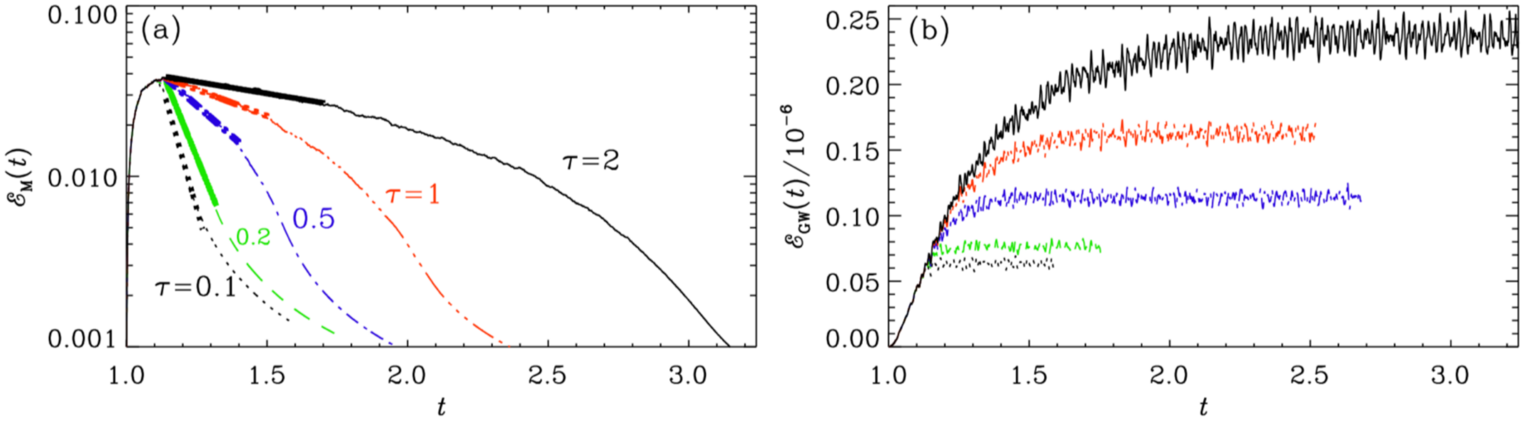

Gravitational wave energy cares mostly about peak energy

Helicity matters

kin driving

mag driven

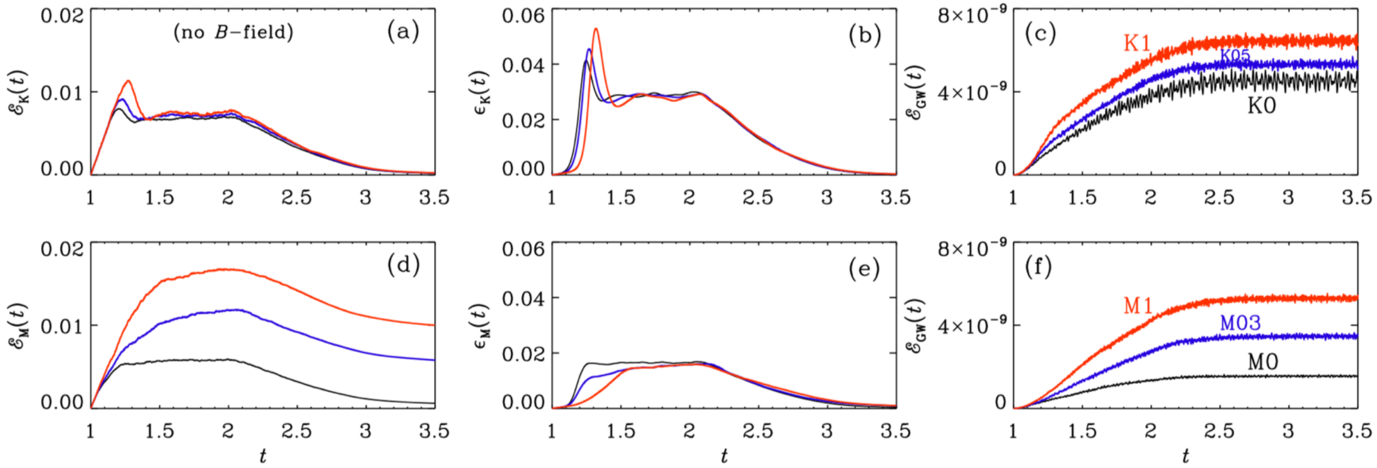

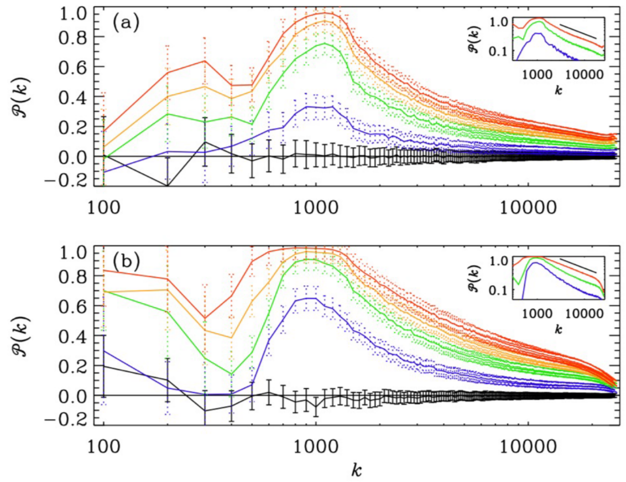

Spectral correspondence invalid for driven fields

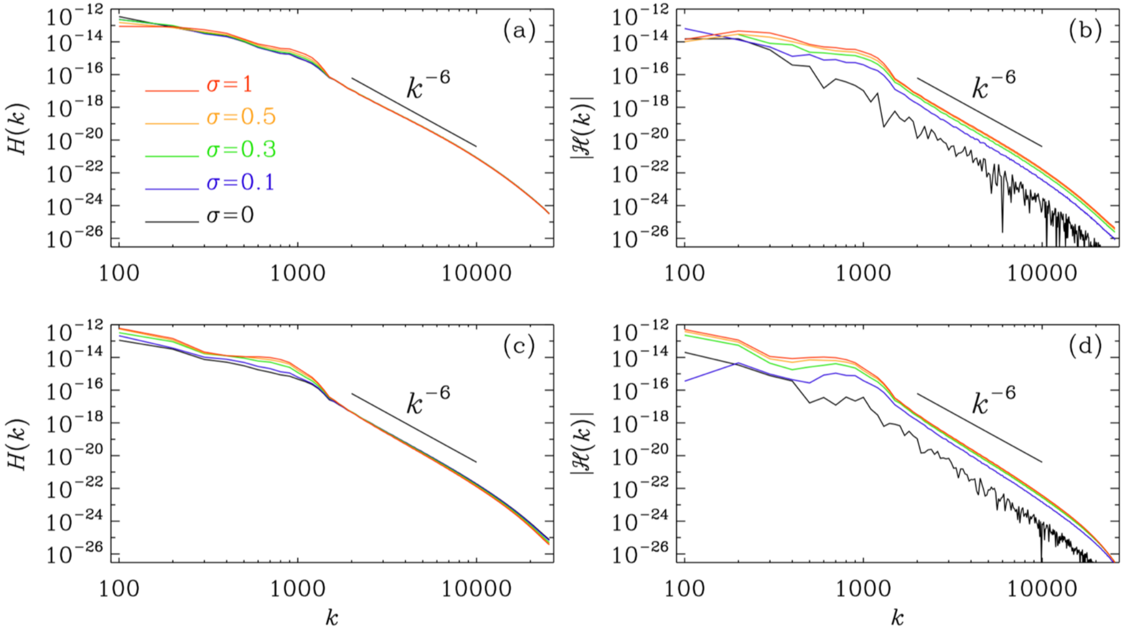

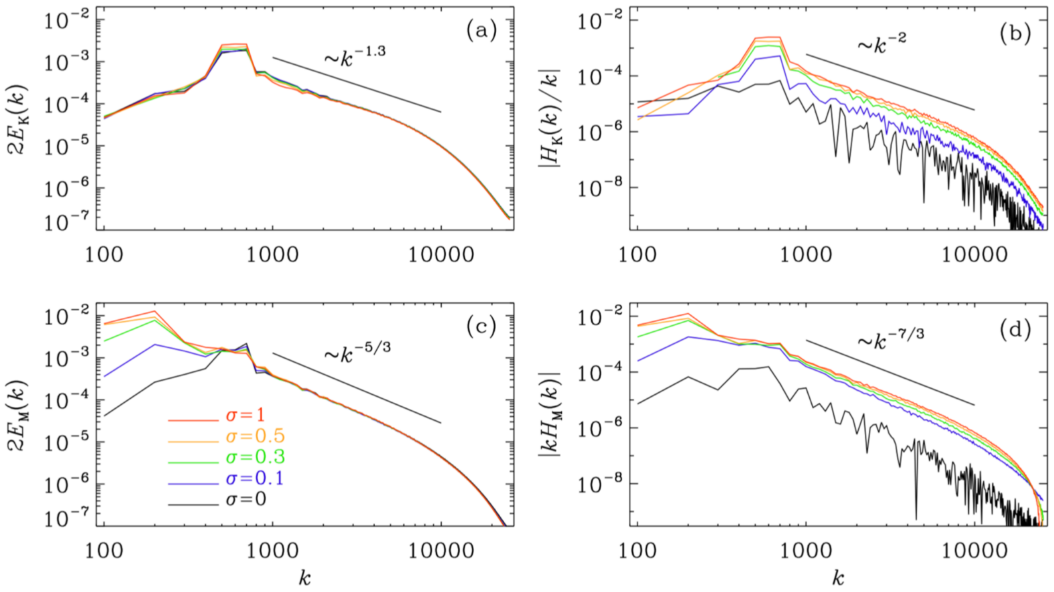

Importance of time dependence during magnetogenesis

Acoustic peak

- Acoustic peak grows with time
  - Linear in time
  - Best when no expansion
  - Extended sound shell model
- Flat background
  - Stays at the same level
  - Expands to the left
- Very steep k^9 slope

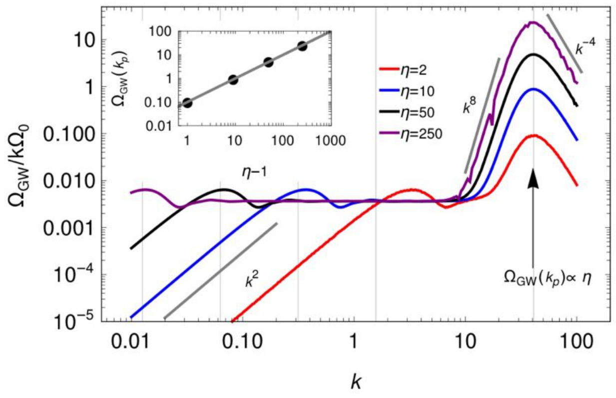

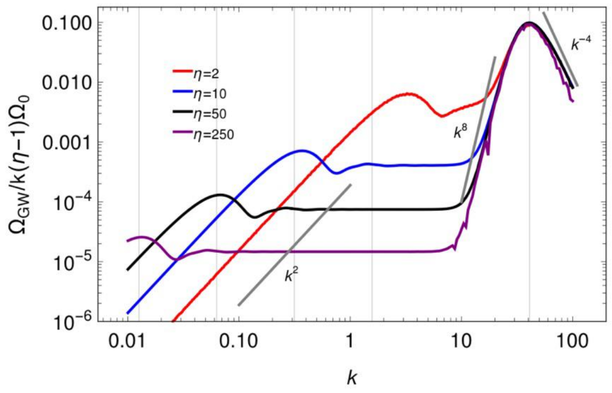

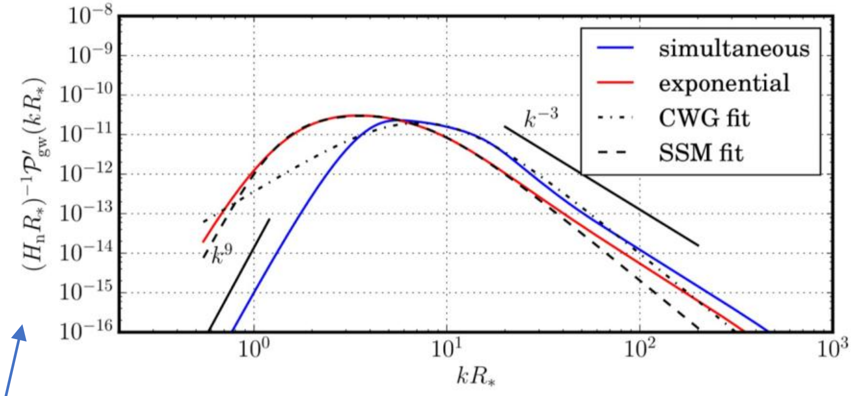

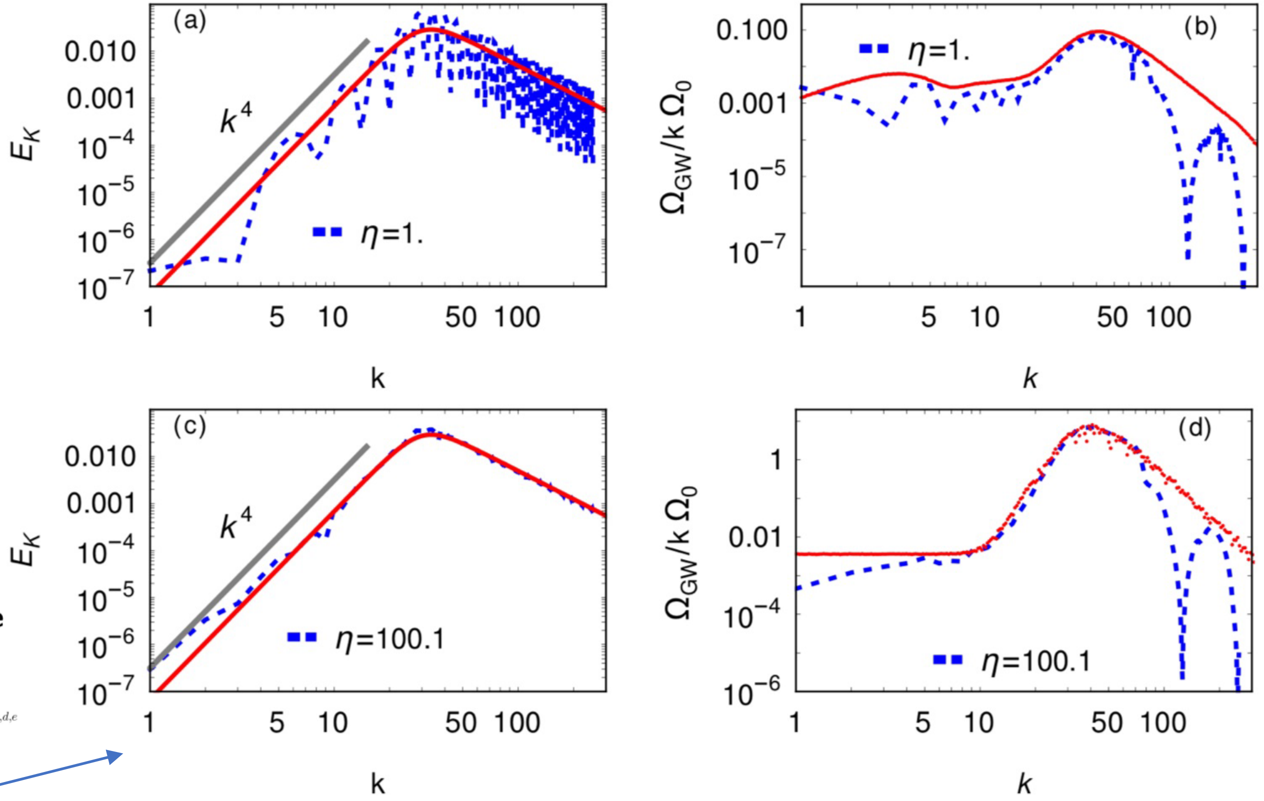

Gravitational waves from first order cosmological phase transitions in the Sound Shell Model

Mark Hindmarsh[a,b] and Mulham Hijazi[c]

Shallow relic gravitational wave spectrum with acoustic peak

Ramkishor Sharma,[a,b] Jani Dahl,[c] Axel Brandenburg[a,b,d,e] and Mark Hindmarsh[c,f]

Larger efficiency from magnetogenesis (chiral magn effect)

Rogachevskii, Boyarsky+17

Chiral magnetic effect (CME), use [μ_5]=[k]

$$\frac{\partial \boldsymbol{B}}{\partial t} = \boldsymbol{\nabla} \times [\boldsymbol{u} \times \boldsymbol{B} + \eta(\mu_5 \boldsymbol{B} - \boldsymbol{J})], \quad \boldsymbol{J} = \boldsymbol{\nabla} \times \boldsymbol{B}$$

$$\frac{D\mu_5}{Dt} = -\lambda\, \eta(\mu_5 \boldsymbol{B} - \boldsymbol{J}) \cdot \boldsymbol{B} + D_5 \nabla^2 \mu_5 - \Gamma_{\rm f} \mu_5$$

$$v_\lambda = \mu_{50}/\lambda^{1/2}, \qquad v_\mu = \mu_{50}\eta.$$

$$\eta k_1 < v_\mu < v_\lambda \quad \text{(regime I)},$$

$$\eta k_1 < v_\lambda < v_\mu \quad \text{(regime II)},$$

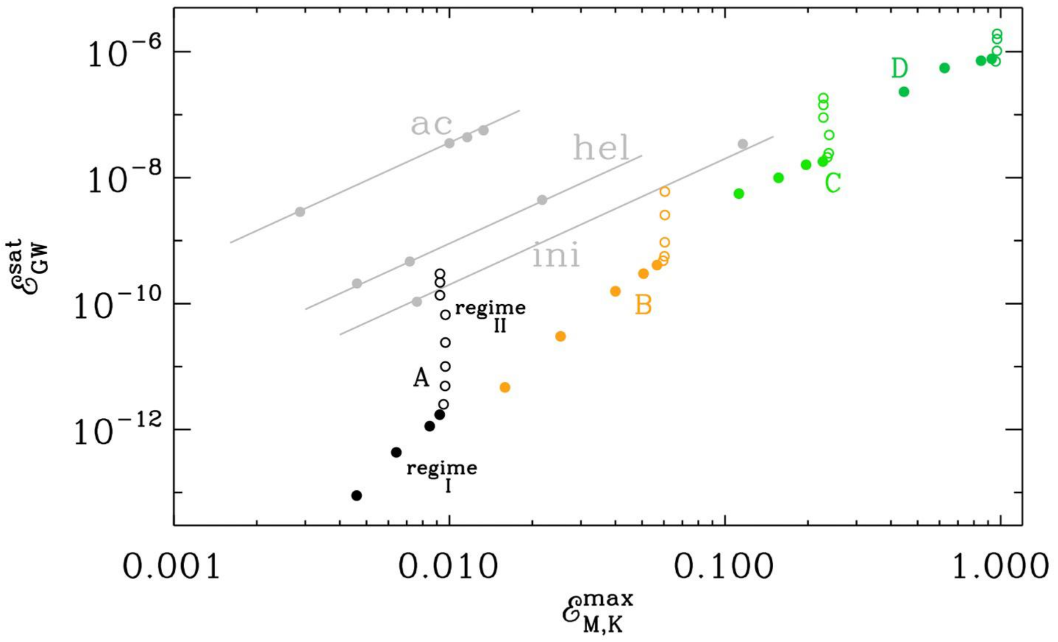

Brandenburg+21

- Regime II: is more resistive → unrealistic, but large GW energies
- Regime I: → realistic, but small scales & less GW energy

Inflationary magnetogenesis

- Early Universe Turbulence
  - Source of gravitational waves
  - Information from young universe
- Magnetogenesis
  - Inflation/reheating
  - No particles yet, no conductivity
  - Coupling with electromagn field

$$f^2 F_{\mu\nu} F^{\mu\nu}$$

  - Breaking of conformal invariance
  - Quantum fluct → field stretched

$$\tilde{\mathbf{A}}'' + \left(\mathbf{k}^2 - \frac{f''}{f}\right)\tilde{\mathbf{A}} = 0,$$

$$\tilde{h}''_{+/\times} + \left(\mathbf{k}^2 - \frac{a''}{a}\right)\tilde{h}_{+/\times} = \frac{6}{a}\tilde{T}_{+/\times},$$

Lattice simulations of axion-U(1) inflation: gravitational waves, magnetic fields, and black holes

Ramkishor Sharma,[a] Axel Brandenburg,[b,c,d,e]
Kandaswamy Subramanian,[f,g] and Alexander Vikman[a]

$$\phi'' + 2\mathcal{H}\phi' - \nabla^2\phi + a^2\frac{dV}{d\phi} = \frac{\alpha}{f}\frac{1}{a^2}\mathbf{E}\cdot\mathbf{B},$$

$$\mathbf{A}'' - \boldsymbol{\nabla}A_0' - \nabla^2\mathbf{A} + \boldsymbol{\nabla}(\boldsymbol{\nabla}\cdot\mathbf{A}) - \frac{\alpha}{f}\left(\phi'\mathbf{B} + \boldsymbol{\nabla}\phi\times\mathbf{E}\right) = 0,$$

Contributions to stress:

$$T_{ij} = -B_iB_j - E_iE_j + a^2\partial_i\phi\partial_j\phi + \ldots$$

Inflationary growth & magnetic decay

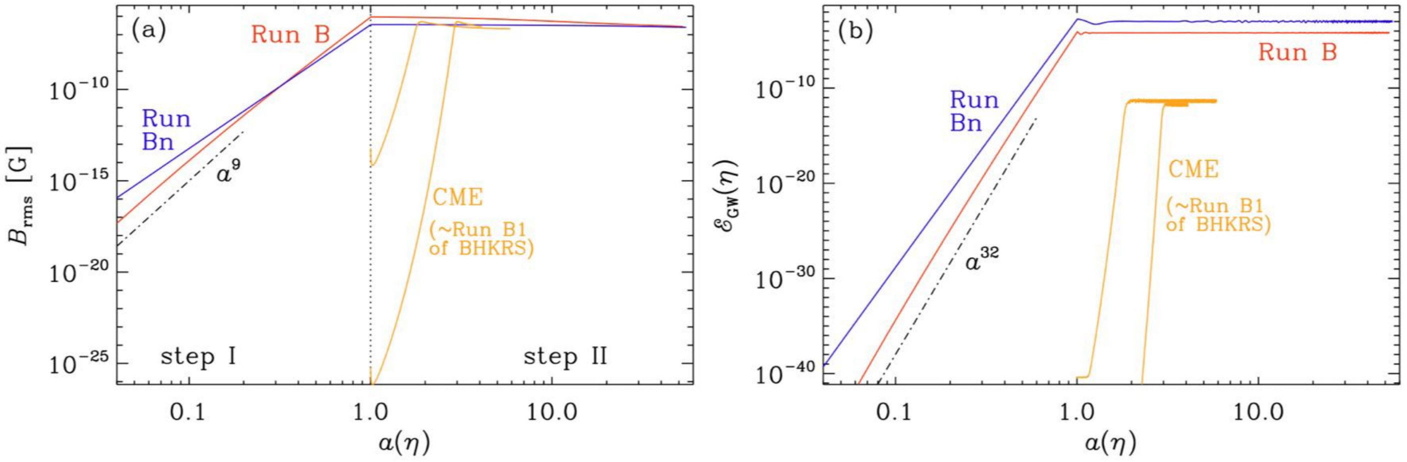

Inflationary growth: electric, magnetic, and GW grow

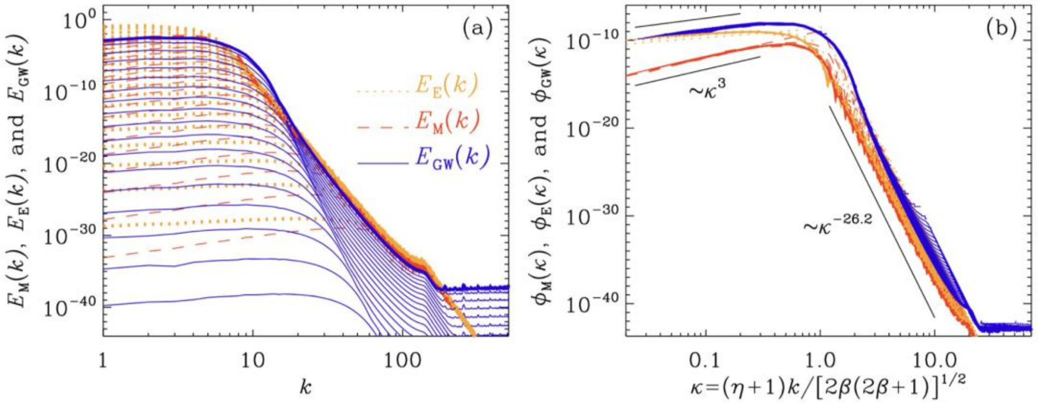

Lorentz force drives smaller scales: surprisingly weak

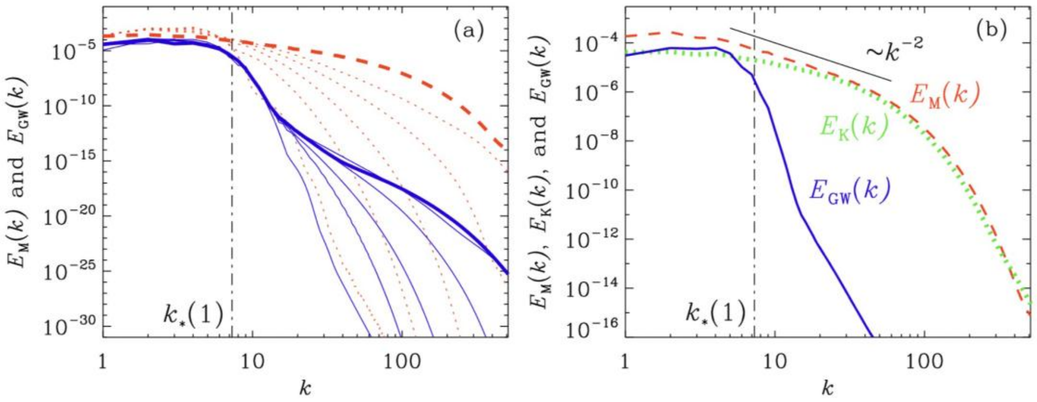

Circular polarization in chiral inflationary magnetogenesis

$$\iota f^2 F_{\mu\nu} {}^*F^{\mu\nu}$$

$$f(a) = a^{-\beta}, \quad \text{where } a = (\eta + 1)^2/4$$

$$\tilde{A}''_{\pm} + \left(k^2 \pm 2\iota k \frac{f'}{f} - \frac{f''}{f}\right)\tilde{A}_{\pm} = 0,$$

$$\frac{f'}{f} = -\frac{2\beta}{\eta + 1}, \qquad \frac{f''}{f} = \frac{2\beta(2\beta+1)}{(\eta+1)^2}.$$

- Step I: spectra peaked
- Step II: Inverse cascade
- GW: circularly polarized

$$\mathcal{P}(k) = \int 2\,\mathrm{Im}\,\tilde{h}_+ \tilde{h}_\times^*\, k^2 \mathrm{d}\Omega_k \bigg/ \int \left(|\tilde{h}_+|^2 + \tilde{h}_\times|^2\right) k^2 \mathrm{d}\Omega_k$$

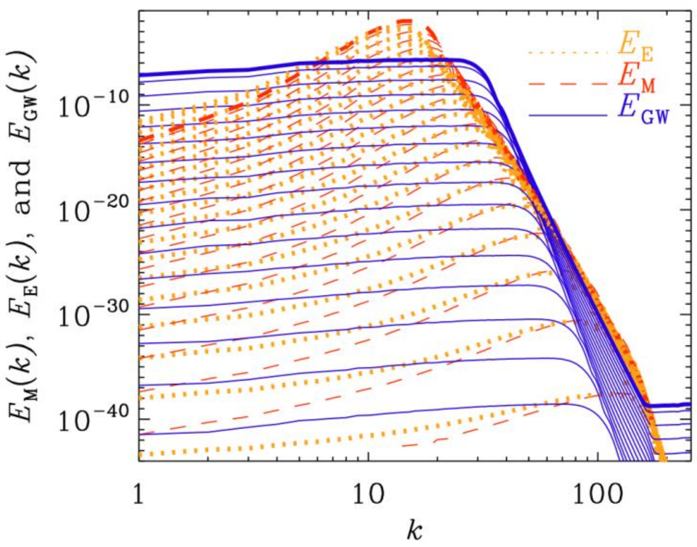

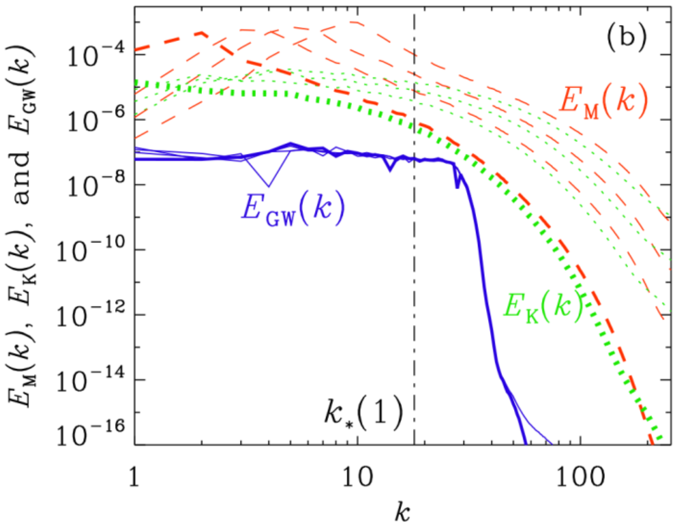

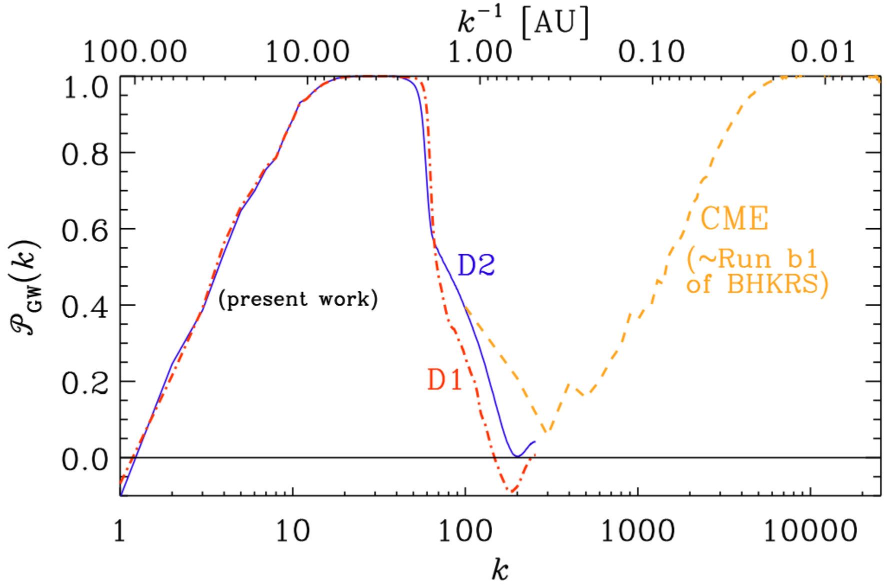

Helical field from CME or inflation: Always ~100% circular polarized

No small scales in GW field

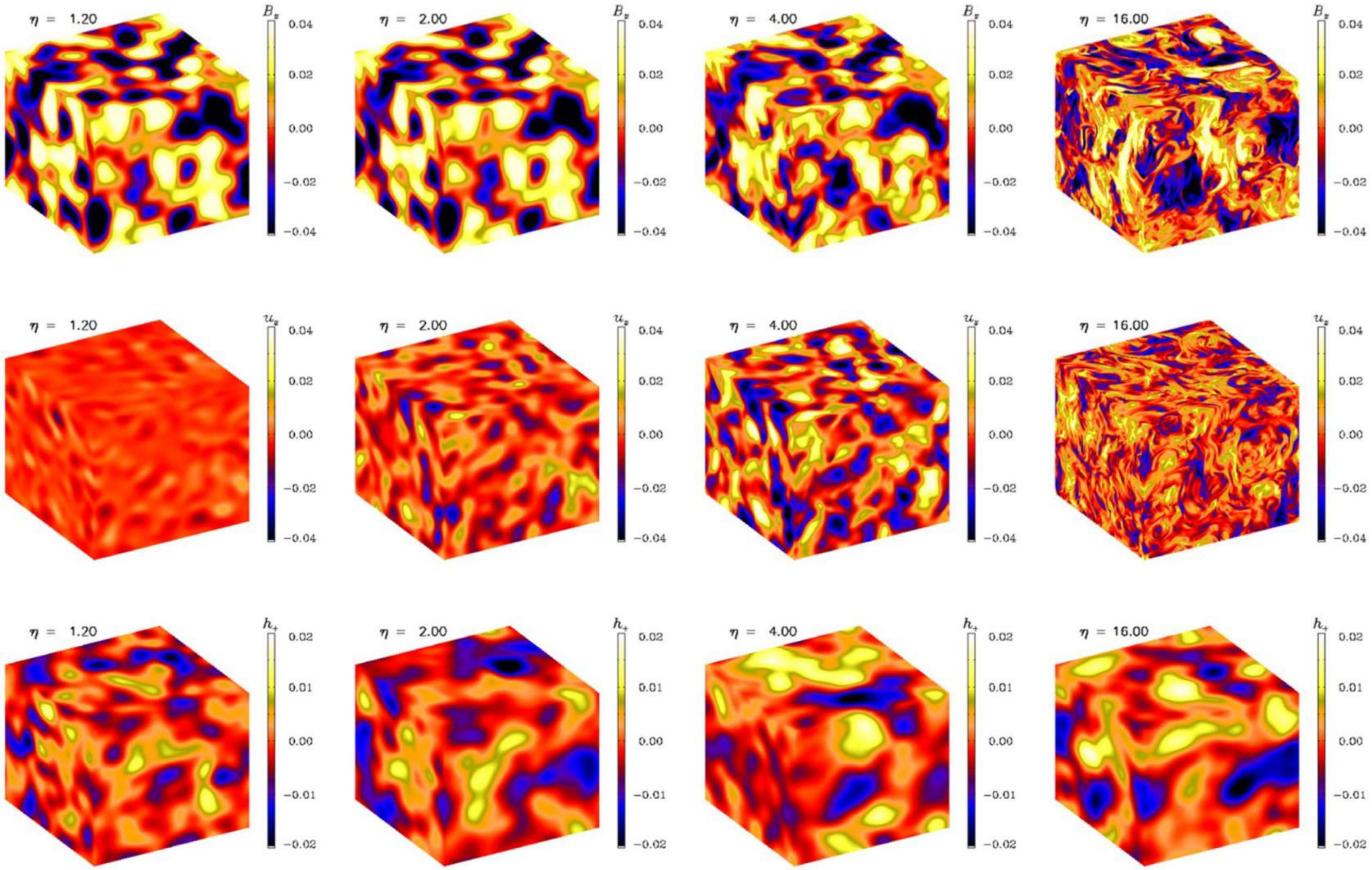

Limit of "ideal" MHD

Perfect conductivity
—> No dissipation

$$\langle \boldsymbol{J} \cdot \boldsymbol{E} \rangle = \langle \boldsymbol{J}^2/\sigma \rangle + \langle \boldsymbol{u} \cdot (\boldsymbol{J} \times \boldsymbol{B}) \rangle$$

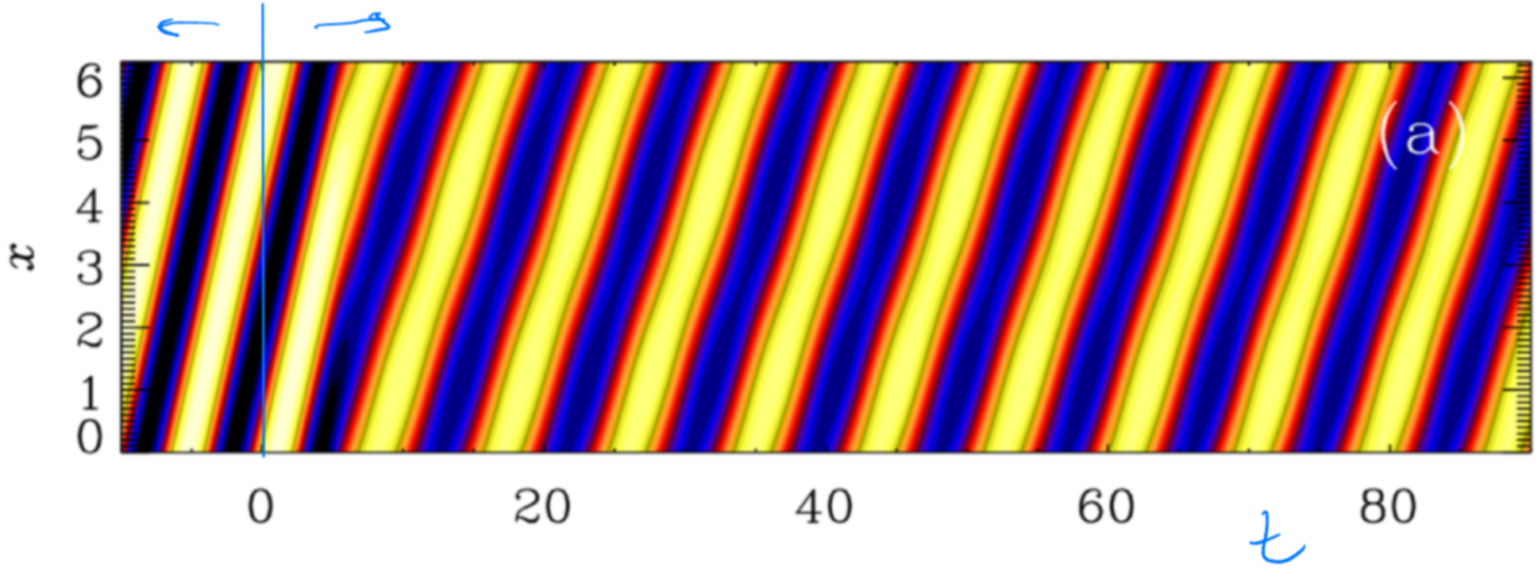

Vacuum, zero conductivity
—> also no dissipation

t<0 electromagnetic waves
t>0 Alfven waves

$$\frac{\mathrm{d}}{\mathrm{d}t}\left(\left\langle \boldsymbol{B}^2/2\mu_0\right\rangle + \left\langle \epsilon_0 \boldsymbol{E}^2/2\right\rangle\right) = -\langle \boldsymbol{J}\cdot\boldsymbol{E}\rangle$$

$$\boldsymbol{J} = \sigma\left(\boldsymbol{E} + \boldsymbol{u}\times\boldsymbol{B}\right)$$

$$\boldsymbol{E} = \boldsymbol{J}/\sigma - \boldsymbol{u}\times\boldsymbol{B}$$

$$\langle \boldsymbol{J}\cdot\boldsymbol{E}\rangle = \langle \boldsymbol{J}^2/\sigma\rangle + \langle \boldsymbol{u}\cdot(\boldsymbol{J}\times\boldsymbol{B})\rangle$$

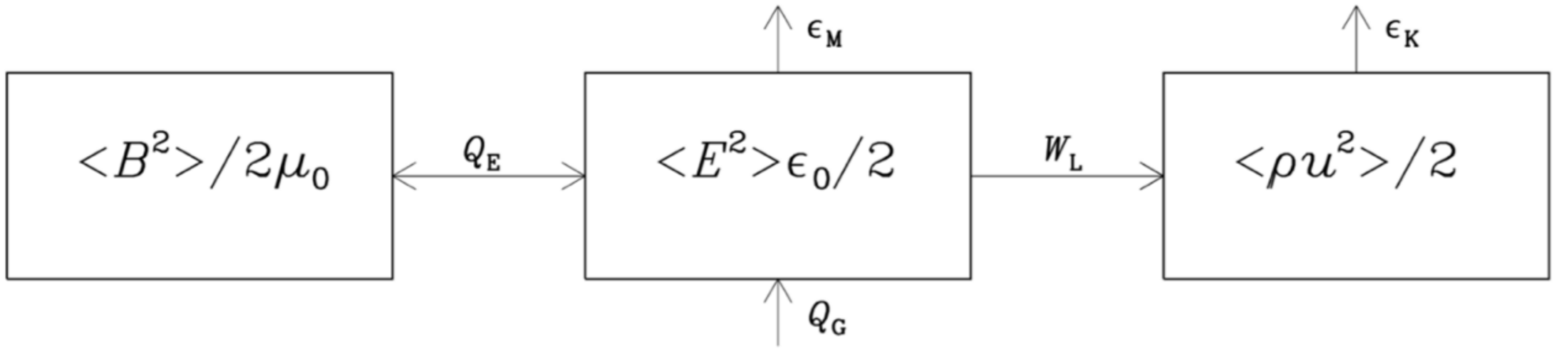

Work by Lorentz force

MHD after inflation

$$f^2 F^{\mu\nu} F_{\mu\nu}$$

$$f \propto a^{-\beta}$$

Sharma+17

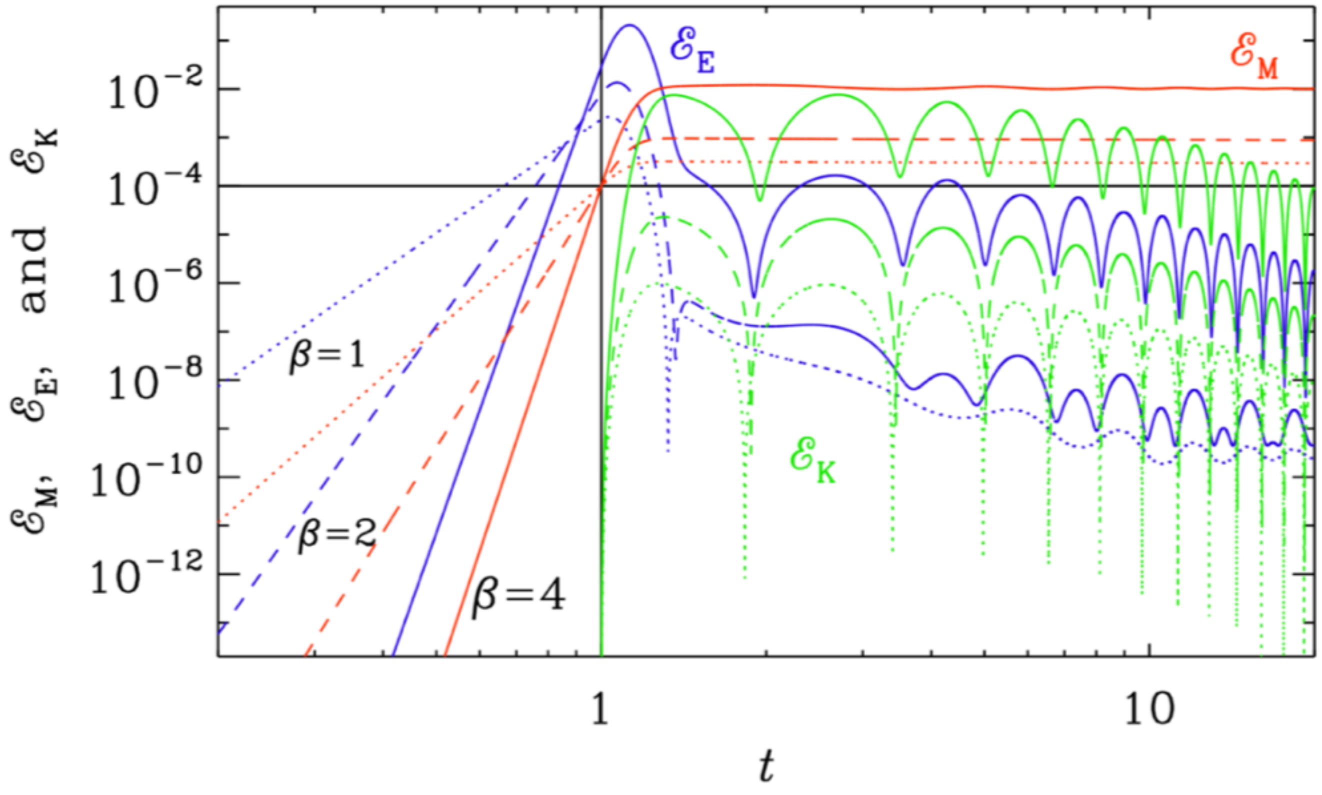

Loss of electric energy —> Gain of kinetic and magnetic energy

$$\mathcal{E}_M \equiv \langle \boldsymbol{B}^2/2\mu_0 \rangle, \quad \mathcal{E}_E \equiv \langle \epsilon_0 \boldsymbol{E}^2/2 \rangle, \quad \text{and} \quad \mathcal{E}_K \equiv \langle \rho \boldsymbol{u}^2/2$$

NORDITA-2025-030

Schwinger effect in axion inflation on a lattice

Oksana Iarygina,[1,2,*] Evangelos I. Sfakianakis,[3,4,†] and Axel Brandenburg[1,2,5,6,‡]

arXiv:2506.20538v1 [astro-ph.CO] 25 Jun 2025

EoM

$$\partial_\tau^2\phi + 2\mathcal{H}\partial_\tau\phi - \nabla^2\phi + a^2\frac{dV}{d\phi} = \frac{\alpha}{a^2 f}\boldsymbol{E}\cdot\boldsymbol{B},$$

$$\partial_\tau\boldsymbol{E} - \mathrm{rot}\,\boldsymbol{B} + \frac{\alpha}{f}\left(\partial_\tau\phi\boldsymbol{B} + \nabla\phi\times\boldsymbol{E}\right) + \boldsymbol{J} = 0,$$

$$\nabla\cdot\boldsymbol{E} = -\frac{\alpha}{f}\nabla\phi\cdot\boldsymbol{B}, \quad \nabla\cdot\boldsymbol{B} = 0,$$

$$\partial_\tau\boldsymbol{B} + \mathrm{rot}\,\boldsymbol{E} = 0,$$

$$\mathcal{H}^2 = \frac{8\pi}{3m_{\mathrm{Pl}}^2}a^2\left(\rho_\phi + \rho_E + \rho_B + \rho_\chi\right),$$

$$\rho_\phi = \left\langle(\partial_\tau\phi)^2/2a^2 + (\nabla\phi)^2/2a^2 + V\right\rangle$$

$$V(\phi) = \tfrac{1}{2}m^2\phi^2 \qquad m = 1.04\times10^{-6}\,m_{\mathrm{Pl}}.$$

$$\partial_\tau\rho_\chi + 4\mathcal{H}\rho_\chi = \frac{1}{a^3}\left(\langle\sigma_E\rangle\langle\boldsymbol{E}^2\rangle + \langle\sigma_B\rangle\langle\boldsymbol{E}\cdot\boldsymbol{B}\rangle\right)$$

Ambiguity in choices

Electric, magnetic, mixed pictures

$$\boldsymbol{J} = \sigma_E\boldsymbol{E}, \quad \sigma_E = \frac{(e|Q|)^3}{6\pi^2\mathcal{H}}|B|\coth\left(\frac{\pi B}{E}\right), \tag{8}$$

$$\boldsymbol{J} = \sigma_B\boldsymbol{B}, \quad \sigma_B = \frac{(e|Q|)^3}{6\pi^2\mathcal{H}}\mathrm{sign}(\boldsymbol{E}\cdot\boldsymbol{B})\,E\coth\left(\frac{\pi B}{E}\right), \tag{9}$$

$$\boldsymbol{J} = \sigma_E\boldsymbol{E} + \sigma_B\boldsymbol{B}, \tag{10}$$

All give the same current

$$J = \frac{(e|Q|)^3}{6\pi^2\mathcal{H}}E|B|\coth\left(\frac{\pi|B|}{E}\right)e^{-\frac{\pi m^2 a^2}{e|Q|E}}$$

Validity of $\mathcal{E}_{\rm GW}^{\rm sat} \approx (q\mathcal{E}_{\rm M}^{\rm max}/k_{\rm peak})^2$

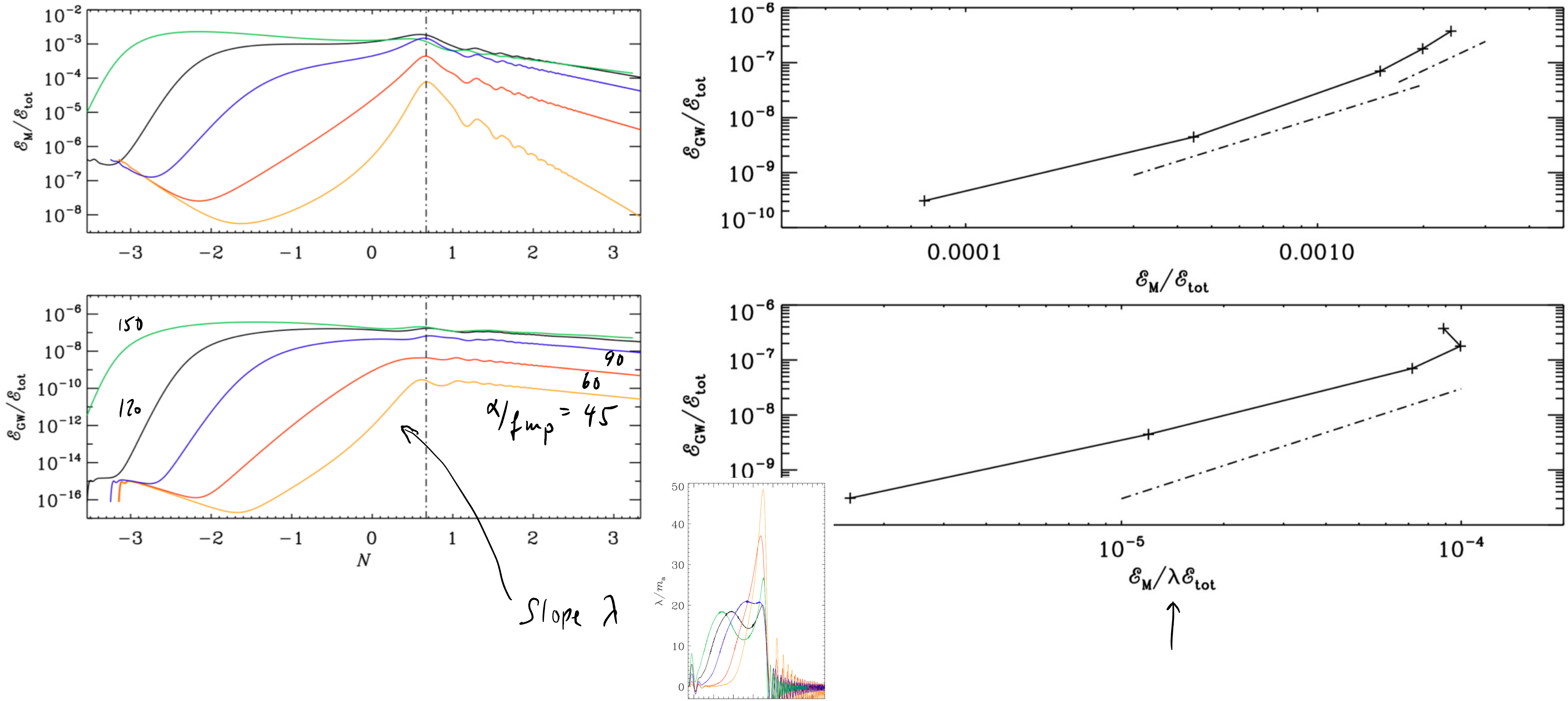

GW energy is weak compared to case without Schwinger

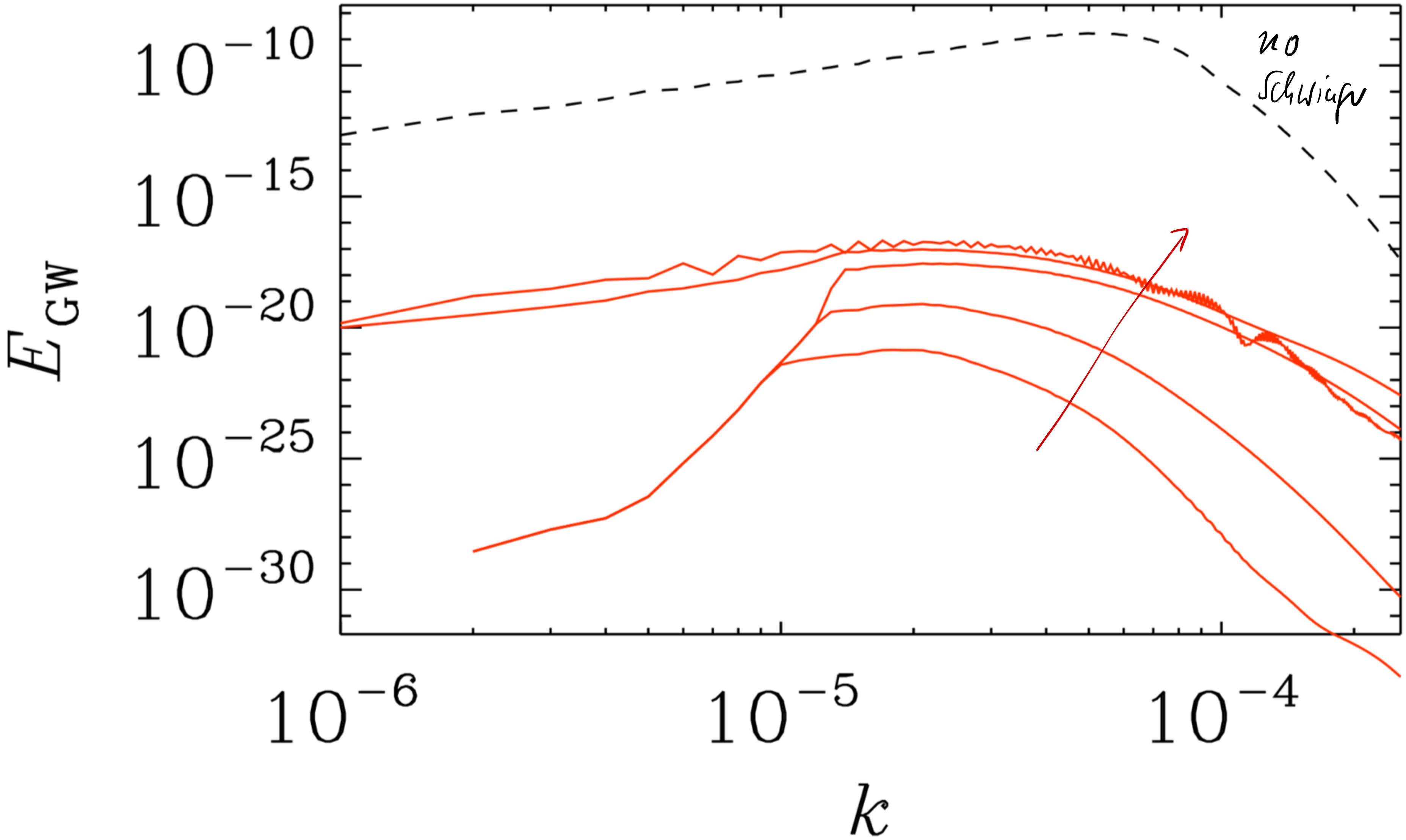

JOSS
The Journal of Open Source Software

The Pencil Code, a modular MPI code for partial differential equations and particles: multipurpose and multiuser-maintained

The Pencil Code Collaboration[1], **Axel Brandenburg**[1, 2, 3], **Anders Johansen**[4], **Philippe A. Bourdin**[5, 6], **Wolfgang Dobler**[7], **Wladimir Lyra**[8], **Matthias Rheinhardt**[9], **Sven Bingert**[10], **Nils Erland L. Haugen**[11, 12, 1], **Antony Mee**[13], **Frederick Gent**[9, 14], **Natalia Babkovskaia**[15], **Chao-Chin Yang**[16], **Tobias Heinemann**[17], **Boris Dintrans**[18], **Dhrubaditya Mitra**[1], **Simon Candelaresi**[19], **Jörn Warnecke**[20], **Petri J. Käpylä**[21], **Andreas Schreiber**[15], **Piyali Chatterjee**[22], **Maarit J. Käpylä**[9, 20], **Xiang-Yu Li**[1], **Jonas Krüger**[11, 12], **Jørgen R. Aarnes**[12], **Graeme R. Sarson**[14], **Jeffrey S. Oishi**[23], **Jennifer Schober**[24], **Raphaël Plasson**[25], **Christer Sandin**[1], **Ewa Karchniwy**[12, 26], **Luiz Felipe S. Rodrigues**[14, 27], **Alexander Hubbard**[28], **Gustavo Guerrero**[29], **Andrew Snodin**[14], **Illa R. Losada**[1], **Johannes Pekkilä**[9], and **Chengeng Qian**[30]

DOI: 10.21105/joss.02807

Software

- Review
- Repository
- Archive

Editor: Arfon Smith

Reviewers:

- @zingale
- @rtfisher

24 years of Pencil Code

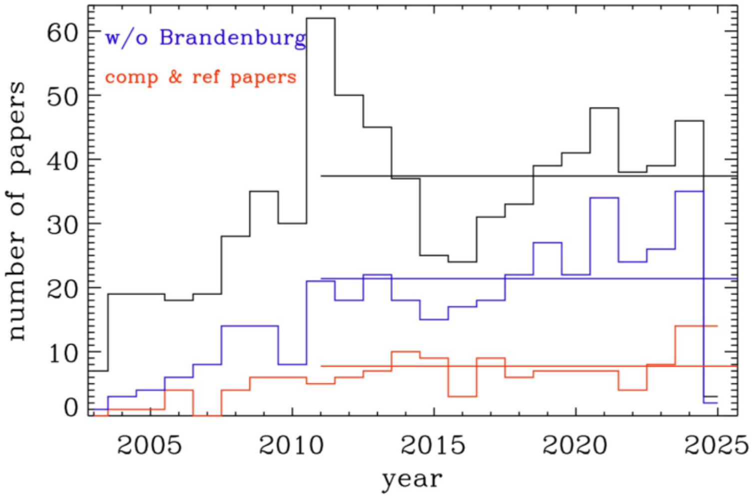

High-level functionality

An idea about the range of available modules can be obtained by inspecting the examples under pencil-code/samples/. Those are low resolution versions related to applications published in the literature. Some of the run directories of actual production runs are published through Zenodo. Below a list of method papers that describe the various applications and tests:

- Coagulation and condensation in turbulence (Johansen et al., 2008; Li et al., 2017),
- Radiative transfer (Barekat & Brandenburg, 2014; A. Brandenburg & Das, 2020; Heinemann et al., 2006),
- Chiral magnetic effect in relativistic plasmas (Schober et al., 2018),
- Primordial gravitational waves (Roper Pol et al., 2020),
- Modeling homochirality at the origin of life (Axel Brandenburg, 2019; A. Brandenburg & Multamäki, 2004),
- Modeling of patterned photochemical systems (Emond et al., 2012),
- Gaseous combustion and detonation (Babkovskaia et al., 2011; Krüger et al., 2017; Zhang et al., 2020),
- Burning particles, resolved or unresolved (Qian et al., 2020),
- Flows around immersed solid objects (Aarnes et al., 2019, 2020; N. E. L. Haugen & Kragset, 2010),
- Test-field method for turbulent MHD transport (A. Brandenburg et al., 2010; Rheinhardt & Brandenburg, 2010; Warnecke et al., 2018),
- Mean-field MHD (Jabbari et al., 2013; Kemel et al., 2013),
- Spherical shell dynamos and convection (P. J. Käpylä et al., 2020; Mitra et al., 2009),
- Boris correction for coronal physics (Chatterjee, 2020),
- Thermal instability and mixing (C.-C. Yang & Krumholz, 2012),
- Implicit solver for temperature (Gastine & Dintrans, 2008),
- Dust-gas dynamics with mutual drag interaction (C.-C. Yang & Johansen, 2016; Youdin & Johansen, 2007),
- Boundary conditions for the solar atmosphere and HDF5 format (Philippe-A. Bourdin, 2020).

- Flows around immersed solid objects (N. E. L. Haugen & Kragset, 2010),
- Particle clustering in supersonic and subsonic turbulence (Karchniwy et al., 2019; Mattsson et al., 2019),
- Cloud microphysics (Li et al., 2017),
- Planet and planetesimal formation (Johansen et al., 2007; Lyra et al., 2009; Oishi et al., 2007),
- Global simulations of debris disks (Lyra & Kuchner, 2013),
- Stratified shearing box simulations, also with dust (Oishi & Mac Low, 2011; Schreiber & Klahr, 2018; C.-C. Yang et al., 2018),
- Supernova-driven turbulence (Gent et al., 2013),
- Solar dynamo and sunspots (A. Brandenburg, 2005; Heinemann et al., 2007),
- Solar corona above active regions (Bingert & Peter, 2011; P.-A. Bourdin et al., 2013; Chatterjee et al., 2016),
- Fully convective star in a box (Dobler et al., 2006),
- Dynamo wave in spherical shell convection (P. J. Käpylä et al., 2012; Warnecke et al., 2014),
- Convection with Kramers opacity law (P. J. Käpylä et al., 2020; Petri J. Käpylä et al., 2017; P. J. Käpylä, 2019),
- MHD turbulence and cascades (N. E. Haugen et al., 2004),
- Turbulent diffusivity quenching with test fields (A. Brandenburg et al., 2008; Karak et al., 2014).

H=37 people have done > 37 commits

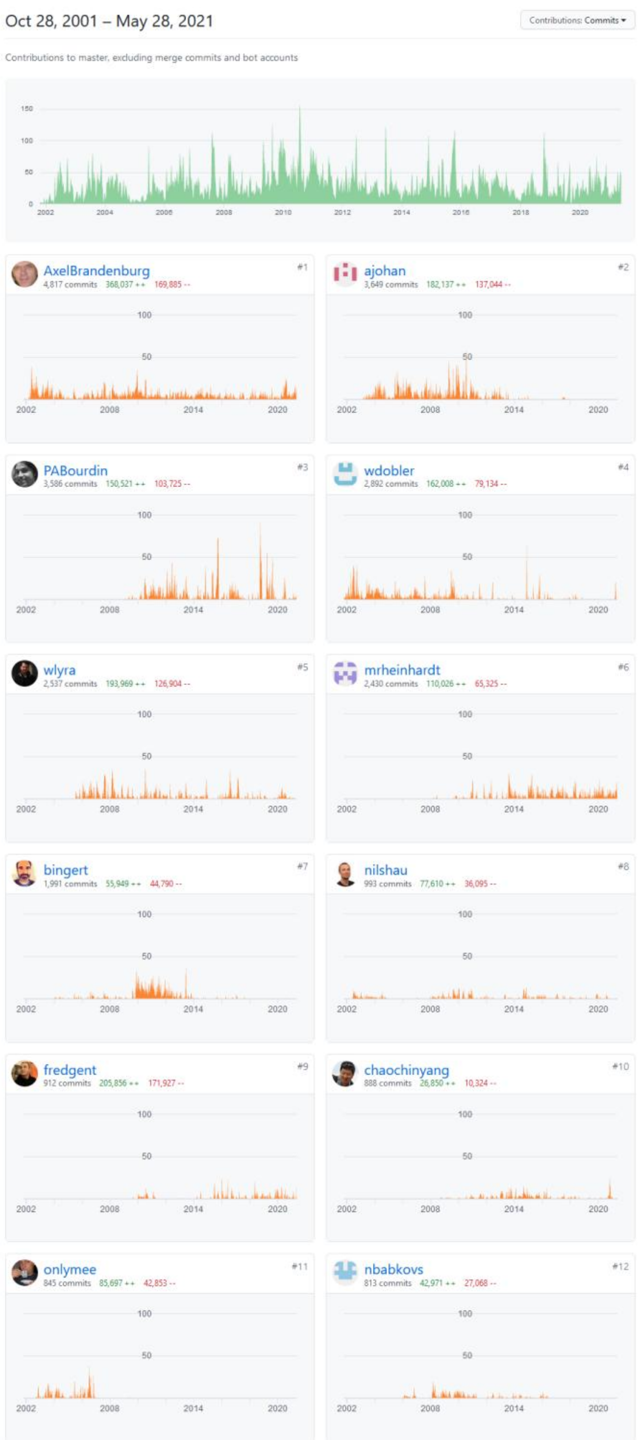

multipurpose

2 Papers by topic

The Pencil Code has been used for the following research topics

1. **Interstellar and intercluster medium as well as early Universe**

   (a) *Interstellar and intercluster medium* (Korpi-Lagg *et al.*, 2024; Elias-López *et al.*, 2024, 2023; Pavaskar *et al.*, 2023; Gent *et al.*, 2023; Brandenburg and Ntormousi, 2022; Maiti *et al.*, 2021; Gent *et al.*, 2021; Li and Mattsson, 2021; Candelaresi and Del Sordo, 2021, 2020; Li and Mattsson, 2020; Brandenburg and Furuya, 2020; Brandenburg and Brüggen, 2020; Gent *et al.*, 2020; Evirgen and Gent, 2019; Evirgen *et al.*, 2019; Seta and Beck, 2019; Rodrigues *et al.*, 2019; Brandenburg, 2019a; Väisälä *et al.*, 2018; Zhang

   (b) *Small-scale dynamos and reconnection* (Kishore and Singh, 2025a; Brandenburg and Ntormousi, 2025; Warnecke *et al.*, 2025; Gent *et al.*, 2024; Zhou and Jingade, 2024; Qazi *et al.*, 2025, 2024; Brandenburg and Larsson, 2023; Warnecke *et al.*, 2023; Gent *et al.*, 2022; Brandenburg *et al.*, 2023c; Zhou *et al.*, 2022; Bhat, 2021; Park and Cheoun, 2021; Santos-Lima *et al.*, 2021; Park, 2020; Pusztai *et al.*, 2020; Rüdiger *et al.*, 2020; Seta *et al.*, 2020; Käpylä, 2019; Bhat *et al.*, 2019; Brandenburg and Rempel, 2019; Brandenburg *et al.*, 2018a; Käpylä *et al.*, 2018; Bhat *et al.*, 2016b; Bhat and Subramanian, 2013; Brandenburg, 2011c; Baggaley *et al.*, 2009, 2010; Schekochihin *et al.*, 2005, 2007; Haugen and Brandenburg, 2004b; Haugen *et al.*, 2003, 2004a,c; Dobler *et al.*, 2003).

   (c) *Primordial magnetic fields and decaying turbulence* (Dehman and Brandenburg, 2025; Vachaspati and Brandenburg, 2024; Brandenburg and Banerjee, 2024; Dwivedi *et al.*, 2024; Brandenburg *et al.*, 2024a, 2023d; Mtchedlidze *et al.*, 2024, 2023, 2022; Bhat *et al.*, 2021; Brandenburg, 2023a, 2020a; Brandenburg *et al.*, 2020b, 2019b; Kahniashvili *et al.*, 2020; Brandenburg *et al.*, 2018b; Trivedi *et al.*, 2018; Brandenburg *et al.*, 2017d; Brandenburg and Kahniashvili, 2017; Kahniashvili *et al.*, 2017; Reppin and Banerjee, 2017; Park, 2017; Osano and Adams, 2017; Adams and Osano, 2016; Osano and Adams, 2016b,a; Kahniashvili *et al.*, 2016; Brandenburg *et al.*, 2015; Adams and Osano, 2014; Kahniashvili *et al.*, 2012, 2013; Tevzadze *et al.*, 2012; Candelaresi and Brandenburg, 2011a; Kahniashvili *et al.*, 2010; Del Sordo *et al.*, 2010; Christensson *et al.*, 2005; Yousef *et al.*, 2004).

   (d) *Relic gravitational waves & axions* (Sharma *et al.*, 2025c; Brandenburg *et al.*, 2024b,c; Iarygina *et al.*, 2024; Sharma *et al.*, 2023; He *et al.*, 2023; Roper Pol, 2022; Sharma and Brandenburg, 2022; AlbertoRoper, 2022; Kahniashvili *et al.*, 2022; Roper Pol, 2021; Roper Pol *et al.*, 2022b; He *et al.*, 2021b,a; Brandenburg *et al.*, 2021b,d; Brandenburg and Sharma, 2021; Brandenburg *et al.*, 2021a,c; Kahniashvili *et al.*, 2021; Roper Pol *et al.*, 2020b,a).

2. **Planet formation and inertial particles**

   (a) *Planet formation* (Rice *et al.*, 2025; Eriksson *et al.*, 2025; Shi *et al.*, 2025; Baehr *et al.*, 2022; Yang and Zhu, 2021; Raettig *et al.*, 2021; Baehr and Zhu, 2021b,a; Zhu and Yang, 2021; Klahr and Schreiber, 2021, 2020; Yang and Zhu, 2020; Eriksson *et al.*, 2020; Gerbig *et al.*, 2020; Castrejon *et al.*, 2019; Baehr and Klahr, 2019; McNally *et al.*, 2018; Schreiber and Klahr, 2018; Hernandez *et al.*, 2019; Manser *et al.*, 2019; Yang *et al.*, 2018; Rice and Nayakshin, 2018; Richert *et al.*, 2018; Kuchner *et al.*, 2018;

3. **Accretion discs and shear flows**

   (a) *Accretion discs and shear flows* (Meftah, 2025; Lyra *et al.*, 2024; Sengupta *et al.*, 2024; Cañas *et al.*, 2024; Zhou, 2024; Mondal and Bhat, 2023; Meftah, 2023; Tharakkal *et al.*,

   (a) *Coronal heating and coronal mass ejections* (Kishore and Singh, 2025a,b; Singh *et al.*, 2025; Vemareddy, 2024; Kesri *et al.*, 2024; Maity *et al.*, 2024b; Dey *et al.*, 2024; Vemareddy *et al.*, 2024; Zhang *et al.*, 2023; Dey *et al.*, 2022; Chatterjee and Dey, 2022; Jakab and Brandenburg, 2021; Zhuleku *et al.*, 2021; Adrover-González and Terradas,

   (b) *Large-scale dynamos, helical turbulence, and catastrophic quenching* (Brandenburg *et al.*, 2025b; Brandenburg and Vishniac, 2025; Rogachevskii *et al.*, 2025; Brandenburg *et al.*, 2025a; Mondal *et al.*, 2025; Shchutskyi *et al.*, 2025; Hidalgo *et al.*, 2025; Zhou and Lai,

   (b) *Hydrodynamic and MHD instabilities* (Oliveira *et al.*, 2021; Del Sordo *et al.*, 2012; Chatterjee *et al.*, 2011b,c; Bejarano *et al.*, 2011; Brandenburg and Rüdiger, 2005; Brandenburg *et al.*, 2004c; Brandenburg, 2003).

   (c) *Chiral MHD* (Schober *et al.*, 2024b,a; Brandenburg *et al.*, 2023a,b; Schober *et al.*, 2022a,b, 2020a,b, 2019, 2018; Brandenburg *et al.*, 2017e).

   (d) *Hydrodynamic and MHD turbulence* (Brandenburg and Scannapieco, 2025; Park, 2025; Roper Pol and Salvino Midiri, 2025; Brandenburg *et al.*, 2025c, 2023e; Brandenburg and Boldyrev, 2020; Aiyer *et al.*, 2017; Yokoi and Brandenburg, 2016; Brandenburg and Petrosyan, 2012; Del Sordo and Brandenburg, 2011a,b; Brandenburg and Nordlund, 2011; Haugen and Brandenburg, 2004a, 2006; Brandenburg *et al.*, 2005c; Pearson *et al.*, 2004).

   (e) *Turbulent combustion, front propagation, radiation & ionization* (Yuvraj *et al.*, 2025; Lipatnikov, 2024b; Wang *et al.*, 2024; Ganti *et al.*, 2023; Yuvraj *et al.*, 2023; Lipatnikov and Sabelnikov, 2022, 2023; Karchniwy *et al.*, 2022; Bhatia and De, 2021; Zhang

multiuser-maintained

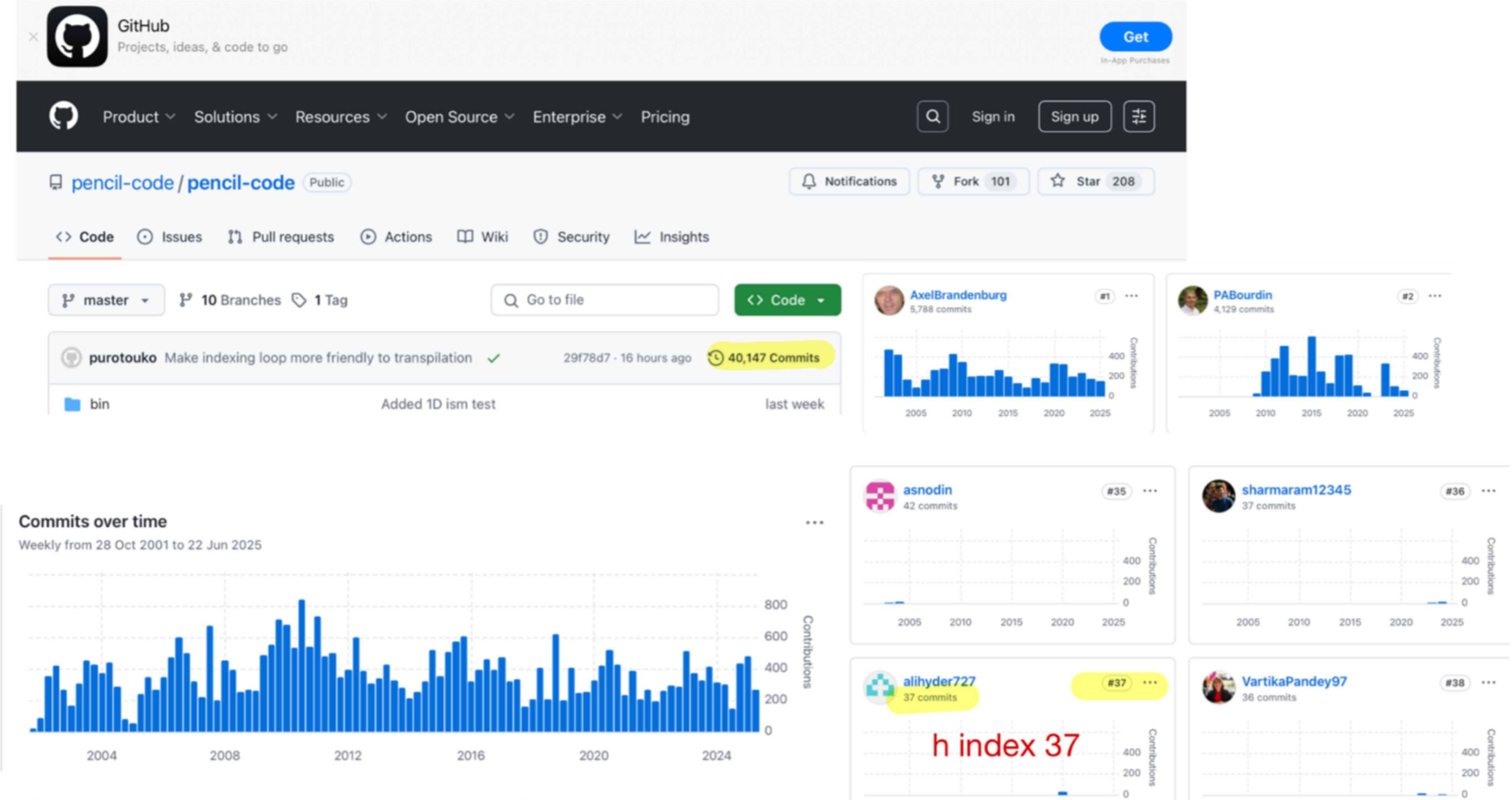

Continuous commits (>40,000) since 2001

Automatic testing: lowers threshold for newcomers

Commits on Jun 23, 2025

- **MR: declaration missing**
  Matthias Rheinhardt committed 3 days ago · ✓ 1 / 1
- **MR: k1_ff -> k1_ff_mag, but k1_ff still in run_pars**
  Matthias Rheinhardt committed 3 days ago · ✗ 0 / 1
- **increase n_pars in gravitational_waves_hTXk**
  ToxPuro committed 4 days ago · ✓ 1 / 1
- **non-rhs kernels of for gravitational_waves_hTXk.f90**
  ToxPuro committed 4 days ago · ✓ 1 / 1

Commits on Jun 21, 2025

- **magnetic.f90: Initialize current to zero, if lohm_evolve=T.**
  AxelBrandenburg committed last week · ✓ 1 / 1
- **initialize lohm_evolve=.false.**
  AxelBrandenburg committed last week · ✓ 1 / 1

Commits on Jun 19, 2025

- **MR: removed uneeded; improved cleaning; comments**
  mrheinhardt committed last week · ✓ 1 / 1
- **MR: back to underscoring: doesn't matter for Linux, is needed for MacOS**
  mrheinhardt committed last week · ✓ 1 / 1

Automatic tests

To ensure reproducibility, the Pencil Code is tested for a number of sample applications. This is important for us in order to make sure certain improvements in some parts of the code do not affect the functionality of other parts. For other users who suspect that a new problem has emerged it could be useful to first see whether this problem also shows up in our own tests. The latest test results for a can be seen online:

level	name	description	time	OK	runs	host	compiler	maintainer
0	minimal	no- & most-modules	minutely	✓	latest (previous)	pencil-code.org	GNU 9.4	Philippe
0+1	basic	same as Travis	minutely	✓	latest (previous)	Norlx51	GNU 13.3	Axel/Philippe
2	normal	without basic	*/*:15	✗	latest (previous)	Norlx51	GNU 13.3	Axel/Philippe
0-2	default	basic + normal	*/2:03	✗	latest (previous)	Norlx65	GNU 13.3	Philippe/Axel
3	extended	without default	*/*:55	✓	latest (previous)	Norlx51	GNU 13.3	Axel/Philippe
0-3	full test	default + extended	*/6:31	⌛	latest (previous)	pencil-code.org	GNU 9.4	Philippe
4	fixme	succeeded before	*/6:45	⌛	latest (previous)	Norlx51	GNU 13.3	Axel/Philippe
5	overlong	runs less often	15:31	🕒	latest (previous)	Norlx65	GNU 13.3	Philippe/Axel
6-9	defective	known to fail	03:31	🕒	latest (previous)	Norlx65	GNU 13.3	Philippe/Axel

Legend: */* means every hour, */6:31 means 31 minutes after full hours divisible by 6.
Status of auto-tests: 🕒 scheduled; ⌛ running; ✗ failed; ✓ succeeded.
Tests are triggered only if there are new updates to the code.

Record for each run

```
fre  6 jun 2025 21:55:19 CEST
Submitted batch job 10468169
10468169  # RUN STARTED on nid001108 fre 6 jun 2025 23:05:50 CEST (SVN Revision: 40552, date of run.x: 2025-06-04 09:44)
10468169  # RUN FINISHED on nid001108 lör 7 jun 2025 22:21:57 CEST (SVN Revision: 40552, date of run.x: 2025-06-04 09:44)

sön  8 jun 2025 23:05:57 CEST
Submitted batch job 10497869
10497869  # RUN STARTED on nid001070 sön 8 jun 2025 23:14:30 CEST (SVN Revision: 40595, date of run.x: 2025-06-07 07:52)
10497869  # RUN FINISHED on nid001070 mån 9 jun 2025 20:49:06 CEST (SVN Revision: 40595, date of run.x: 2025-06-07 07:52)
```

Pencil Code school and user meeting

20–31 Oct 2025
CERN
Europe/Zurich timezone

Enter your search term

1st Pencil Code school on early Universe physics and gravitational waves (Oct 20-24)

The Pencil Code school on early Universe physics and gravitational waves will take place on October 20-24 as part of a two-week CERN TH institute.

The school targets early-career and senior researchers that are interested in learning and developing numerical skills applied to early Universe physics using Pencil Code.

The lectures will cover numerical aspects:

- *Introduction to Pencil Code*
- *Finite-difference schemes for partial differential equations*
- *Post-processing of data with IDL and Python*
- *GPU acceleration of Pencil Code*

as well as applications to particular physics cases with hands-on exercises on:

- *Magnetohydrodynamics of the early Universe*
- *Generation and evolution of primordial magnetic fields*
- *Chiral magnetohydrodynamics*
- *First-order phase transitions*
- *Gravitational wave production*
- *Axion inflation*

Registration is open and will close on ***July 31st***. The school is limited to a maximum of 30 participants.

Participants of the school are encouraged to also participate in the user meeting (Oct 27-31) and need to register separately.

Numerical Experiments

Numerical Experiments, School on Astrophysical Turbulence and Dynamos, ICTP Trieste, 20-30 April 2009.

- LCD workshop2016 (Boulder, 10-12 May 2016)
- MHD course (Stockholm, January 2012)
- Evry Schatzman school'09 in Aussois.
- Solar Physics and MHD course (Stockholm, May 2009)
- Schedule for Trieste, April 2009

September 2009 (PowerPoint Presentation)

Pencil Code home page, Manual, Manual-II, PowerPoint Presentation, https://github.com/pencil-code

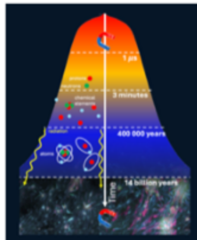

Nordita Winter School 2026 - Cosmological Magnetic Fields: Generation, Observation, and Modeling

12-23 Jan 2026 — Albano Building 3

Enter your search term

- Main Page
- Application
- Timetable
- Slides From Lectures
- Practical Information
  - What is Nordita?
  - Directions to Nordita
  - Directions to BizApartment Hotel

Venue

Registration, 12 Jan. 09:15: Albano Campus, House 3, floor 6 (Nordita building)

Lectures: Room 4205, Conference Center, Albano Campus, House 3, floor 4 (Nordita building)

Workspaces: Use the open desks throughout floor 6 and floor 5 (east).

Coffee: Help yourself to free coffee in Nordita's kitchens on floor 6 and floor 5 (east).

Scope

Magnetic fields are omnipresent in the Universe, we find them in galaxies and galaxy clusers, in filaments and voids of the Large Scale Structure. The presence of magnetic fields in voids hints to the possibility that the initial fields have been generated in the early Universe, within the first

Return to the topic

Connection with hydromagnetics

Growth of conductivity

Growth of magnetic Reynolds number

$v_A = B_{rms}/\sqrt{\rho_\chi}$

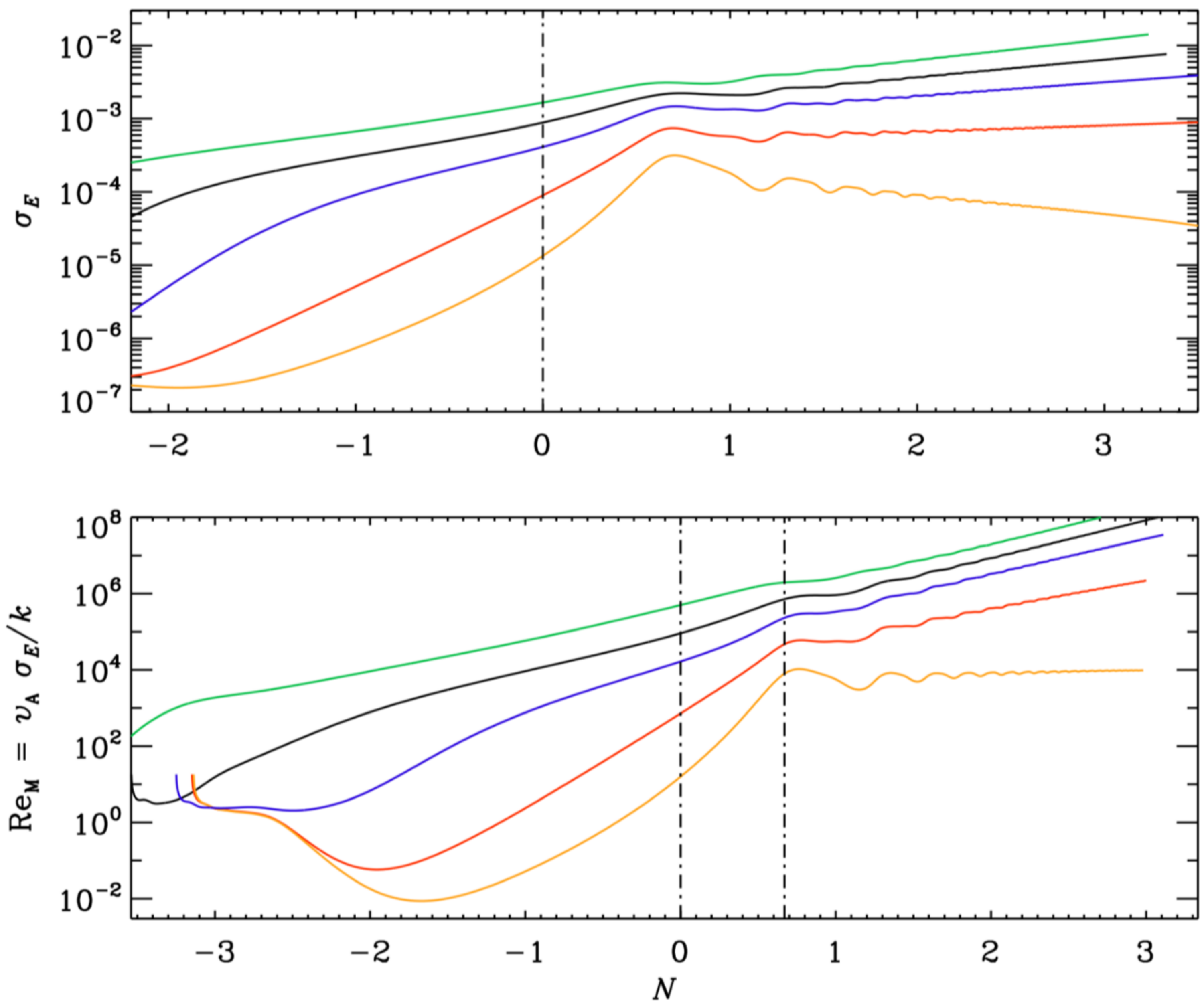

Conclusions

GW field evolution very different from hydro experience

Importance of connecting inflationary magnetogenesis
with radiation era —> Schwinger

Inverse cascade —> magnetic field today

However, GWs map the state at magnetogenesis

Sensitive to detailed time dependence